Cenozoic aridization in Central Eurasia shaped diversification of toad-headed agamas (*Phrynocephalus*; Agamidae, Reptilia)

Evgeniya N Solovyeva [Corresp., 1], Vladimir S Lebedev [1], Evgeniy A Dunayev [1], Roman A Nazarov [1], Anna A Bannikova [2], Jing Che [3, 4], Robert W Murphy [3, 5], Nikolay A Poyarkov [Corresp. 2]

[1] Zoological Museum, Lomonosov Moscow State University, Moscow, Russia

[2] Biological Faculty, Department of Vertebrate Zoology, Lomonosov Moscow State University, Moscow, Russia

[3] State Key Laboratory of Genetic Resources and Evolution, and Center for excellence in Animal Evolution and Genetics, Kunming Institute of Zoology, Chinese Academy of Sciences, Kunming, Yunnan, China

[4] Southeast Asia Biodiversity Research Institute, Chinese Academy of Sciences, Yezin, Nay Pyi Taw, Myanmar

[5] Faculty of Arts and Science, Department of Ecology & Evolutionary Biology, University of Toronto, Toronto, Canada

Corresponding Authors: Evgeniya N Solovyeva, Nikolay A Poyarkov
Email address: anolis@yandex.ru, n.poyarkov@gmail.com

We hypothesize the phylogenetic relationships of the agamid genus *Phrynocephalus* to assess how past environmental changes shaped the evolutionary and biogeographic history of these lizards and especially the impact of paleogeography and climatic factors. *Phrynocephalus* is one of the most diverse and taxonomically confusing lizard genera. As a key element of Palearctic deserts, it serves as a promising model for studies of historical biogeography and formation of arid habitats in Eurasia.

We used 51 samples representing 33 of 40 recognized species of *Phrynocephalus* covering all major areas of the genus. Molecular data included four mtDNA (*COI*, *ND2*, *ND4*, *Cytb*; 2703 bp) and four nuDNA protein-coding genes (*RAG1*, *BDNF*, *AKAP9*, *NKTR*; 4188 bp). AU-tests were implemented to test for significant differences between mtDNA- and nuDNA-based topologies. A time-calibrated phylogeny was estimated using a Bayesian relaxed molecular clock with 9 fossil calibrations. We reconstructed the ancestral area of origin, biogeographic scenarios, body-size and the evolution of habitat preference.

Phylogenetic analyses of nuDNA genes recovered a well-resolved and supported topology. Analyses detected significant discordance with the less-supported mtDNA genealogy. The position of *P. mystaceus* conflicted greatly between the two datasets. MtDNA introgression due to ancient hybridization best explained this result. Monophyletic *Phrynocephalus* contained three main clades: (I) oviparous species from south-western and Middle Asia; (II) viviparous species of Qinghai-Tibetan Plateau (QTP); and (III) oviparous species of the Caspian Basin, Middle and Central Asia. *Phrynocephalus* originated in late Oligocene (26.9 Ma) and modern species diversified during the middle Miocene (14.8–13.5 Ma). The reconstruction of ancestral areas indicated that *Phrynocephalus* originated in Middle East–southern Middle Asia. Body size miniaturization likely occurred early in the history of *Phrynocephalus*. The common ancestor of *Phrynocephalus* probably preferred sandy substrates with the inclusion of clay or gravel.

The time of Agaminae radiation and origin of *Phrynocephalus* in the late Oligocene significantly precedes the landbridge between Afro-Arabia and Eurasia in the Early Miocene. Diversification of *Phrynocephalus* coincides well with the Mid-Miocene Climatic Transition when a rapid cooling of climate drove progressing aridification and the Paratethys Salinity Crisis. These factors likely triggered the spreading of desert habitats in Central Eurasia, which *Phrynocephalus* occupied. The origin of the viviparous Tibetan clade has been associated traditionally with uplifting of the QTP; however, further studies are needed to confirm this. Progressing Late Miocene aridification, the decrease of the Paratethys Basin, orogenesis and

Plio-Pleistocene climate oscillations likely promoted further diversification within *Phrynocephalus*. We discuss *Phrynocephalus* taxonomy in scope of the new analyses.

1   **Cenozoic aridization in Central Eurasia shaped diversification of**

2   **toad-headed agamas (*Phrynocephalus*; Agamidae, Reptilia)**

3   **Evgeniya N. Solovyeva[1]*, Vladimir S. Lebedev[1], Evgeniy A. Dunayev[1], Roman**

4   **A. Nazarov[1], Anna A. Bannikova[2], Jing Che[3,4], Robert W. Murphy[3,5], Nikolay**

5   **A. Poyarkov, Jr.[2],***

7   **1** Zoological Museum, Lomonosov Moscow State University, Moscow, Russia

8   **2** Biological Faculty, Department of Vertebrate Zoology, Lomonosov Moscow State University,

9   Moscow, Russia

10   **3** State Key Laboratory of Genetic Resources and Evolution, and Center for excellence in

11   Animal Evolution and Genetics, Kunming Institute of Zoology, Chinese Academy of Sciences,

12   Kunming, Yunnan, China

13   **4** Southeast Asia Biodiversity Research Institute, Chinese Academy of Sciences, Yezin, Nay Pyi

14   Taw, Myanmar

15   **5** Centre for Biodiversity and Conservation Biology, Royal Ontario Museum, Toronto, Canada

17   **Abstract**

19   We hypothesize the phylogenetic relationships of the agamid genus *Phrynocephalus* to assess

20   how past environmental changes shaped the evolutionary and biogeographic history of these

21   lizards and especially the impact of paleogeography and climatic factors. *Phrynocephalus* is one

22   of the most diverse and taxonomically confusing lizard genera. As a key element of Palearctic

23   deserts, it serves as a promising model for studies of historical biogeography and formation of

24   arid habitats in Eurasia.

25   We used 51 samples representing 33 of 40 recognized species of *Phrynocephalus* covering all

26   major areas of the genus. Molecular data included four mtDNA (*COI*, *ND2*, *ND4*, *Cytb*; 2703 bp)

27   and four nuDNA protein-coding genes (*RAG1*, *BDNF*, *AKAP9*, *NKTR*; 4188 bp). AU-tests were

28   implemented to test for significant differences between mtDNA- and nuDNA-based topologies.

29   A time-calibrated phylogeny was estimated using a Bayesian relaxed molecular clock with 9

30   fossil calibrations. We reconstructed the ancestral area of origin, biogeographic scenarios, body-

31   size and the evolution of habitat preference.

32   Phylogenetic analyses of nuDNA genes recovered a well-resolved and supported topology.

33   Analyses detected significant discordance with the less-supported mtDNA genealogy. The

34   position of *P. mystaceus* conflicted greatly between the two datasets. MtDNA introgression due

35   to ancient hybridization best explained this result. Monophyletic *Phrynocephalus* contained three

36   main clades: (I) oviparous species from south-western and Middle Asia; (II) viviparous species

37   of Qinghai-Tibetan Plateau (QTP); and (III) oviparous species of the Caspian Basin, Middle and

38   Central Asia. *Phrynocephalus* originated in late Oligocene (26.9 Ma) and modern species

39   diversified during the middle Miocene (14.8–13.5 Ma). The reconstruction of ancestral areas

40   indicated that *Phrynocephalus* originated in Middle East–southern Middle Asia. Body size

41   miniaturization likely occurred early in the history of *Phrynocephalus*. The common ancestor of

42   *Phrynocephalus* probably preferred sandy substrates with the inclusion of clay or gravel.

43   The time of Agaminae radiation and origin of *Phrynocephalus* in the late Oligocene significantly

44   precedes the landbridge between Afro-Arabia and Eurasia in the Early Miocene. Diversification

45   of *Phrynocephalus* coincides well with the Mid-Miocene Climatic Transition when a rapid

46   cooling of climate drove progressing aridification and the Paratethys Salinity Crisis. These

47   factors likely triggered the spreading of desert habitats in Central Eurasia, which *Phrynocephalus*

48   occupied. The origin of the viviparous Tibetan clade has been associated traditionally with

49   uplifting of the QTP; however, further studies are needed to confirm this. Progressing Late

50   Miocene aridification, the decrease of the Paratethys Basin, orogenesis and Plio-Pleistocene

51   climate oscillations likely promoted further diversification within *Phrynocephalus*. We discuss

52   *Phrynocephalus* taxonomy in scope of the new analyses.

54   **Introduction**

55   Historical biogeography aims to understand the drivers of speciation including the roles

56   played by plate tectonics and climatic change (Lomolino *et al.* 2006). The eastern part of the

57   Great Palearctic Desert Belt spans from Eastern Europe to eastern China, including Middle Asia

(Kazakhstan, Kyrgyzstan, Uzbekistan, Tajikistan and Turkmenistan) and Central Asia. Middle and Central Asia have one of the oldest desert areas. Desertification started at least 23.8–22.0 million years ago (Ma) (Xia & Hu 1993; Guo *et al.* 2002). Various paleogeographic factors played major roles in the shifting of Central Eurasian climate (Ramstein *et al.* 1997). These include the Miocene retreat of the Paratethys Sea, which stretched over Eurasia 30 Ma (Popov *et al.* 2004, 2009), tectonic activity in Southwest Asia (Whiteman 1978; Weise 1974; Macey *et al.* 1993; Golonka 2004) and the uplifting of the Qinghai-Tibetan Plateau (QTP; Harrison *et al.* 1992, 1995; Ramstein *et al.* 1997; An *et al.* 2001; Molnar 2005). Aridization led to the disappearance of forests and formation of desert ecosystems (Cerling *et al.* 1997; Ma *et al.* 1998) and it intensified in the late Cenozoic following the formation of Asian monsoon climate (Guo *et al.* 2002).

Central Eurasian deserts cradle a rich herpetofauna (Chernov 1948; Chernov 1959; Likhnova 1992; Ananjeva & Tuniyev 1992; Szczerbak 2003). In the late Cenozoic, dramatic climatic changes influenced the origins, diversification and distribution of Central Eurasian reptiles (Macey *et al.* 2000; Melville *et al.* 2009). However, the dearth of phylogenetic and historical biogeographic studies for Central Eurasia does not allow the testing of hypotheses on the biological consequences of Cenozoic climatic events. The reptile fauna of the Central Asian deserts is particularly diverse, yet we still have limited understanding of the drivers of evolution of the constituent species (Melville *et al.* 2009).

The agamid genus *Phrynocephalus* Kaup, 1825, or toad-headed lizards, is one of the most speciose genera in its family. It contains from 28 to over 42 species and spans arid regions from northwestern China to the western side of the Caspian Sea, across the QTP, and Southwest Asia to the Arabian Peninsula (Wermuth 1965; Moody 1980; Barabanov & Ananjeva 2007; Guo & Wang 2007; Uetz & Hosek 2016; Kamali & Anderson 2015) (Fig. 1). The species are ecologically important components of the central Eurasian desert fauna and are highly adapted to sand dunes and stony montane deserts from sea level up to 6400 m a.s.l. (Zhao 1999). They exhibit high levels of variation in ecological and morphological diversity, and the species range from being habitat generalists to specialists (Clemann *et al.* 2008; Dunayev 2009). Oviparous reproduction occurs in lower elevations and yet viviparous species occur on the QTP (Zhao & Adler 1993; Pang *et al.* 2003; Guo & Wang 2007). The involvement of *Phrynocephalus* in so-called "substrate races" leads to much taxonomic confusion (Dunayev 2009), especially because

89   their phylogenetic relationships and historical biogeography remain uncertain. Considerable
90   taxonomic, morphological, allozyme, karyological, osteological, and ethological research has
91   been conducted on the charismatic *Phrynocephalus* of Central Asia (for a brief review on history
92   of phylogenetic studies of the genus *Phrynocephalus* see Supplementary Text File 1). Regardless
93   the phylogenetic and taxonomic relationships within the toad-headed agamas remain
94   controversial and largely unresolved (e.g., Ananjeva & Tuniyev 1992; Arnold 1999; Macey *et al.*
95   1993; Dunayev 1996; Golubev 1993; Zhao & Adler 1993; Pang *et al.* 2003; Ananjeva *et al.* 2006;
96   Solovyeva *et al.* 2011; Solovyeva *et al.*2012; and references therein). Hypothesis-testing can
97   help deduce their origin, diversification and dispersal (Guo & Wang 2007; Melville *et al.* 2009;
98   Solovyeva *et al.* 2014). The most complete genealogic hypothesis obtained up to date
99   (Solovyeva *et al.* 2014) is based entirely on the mtDNA data; several major nodes of the tree
100   have little or no support, so elaboration of a more robust phylogeny based on nuclear markers is
101   needed.

102   Herein, we explore a number of unresolved questions by using both mitochondrial and
103   nuclear DNA markers based for 36 species of *Phrynocephalus* that cover the entire range of the
104   genus. Specifically, we pursue three main objectives: (1) test the hypothesis that the nuDNA and
105   mtDNA trees give compatible estimations of historical relationships; (2) evaluate hypotheses
106   concerning potential climatic and tectonic drivers of speciation by using time-tree ages of each
107   lineage calibrated based on molecular dating and fossils; and (3) reconstruct the ancestral
108   distributions to differentiate among competing scenarios of historical biogeography. Our work
109   offers the most complete taxon sampling to date by including up to 70% of the diversity of the
110   genus. It helps to resolve longstanding phylogenetic and biogeographic issues of Central
111   Eurasian biogeography and provides insights into the biogeographic consequences of Cenozoic
112   aridization.

113

Materials and methods

DNA samples

116   We used 51 samples representing 33 nominal species of *Phrynocephalus* from the
117   collection of Zoological Museum of Moscow University (ZMMU). The primary outgroup
118   included six other Agaminae species from the genera *Agama* Daudin, 1802, *Paralaudakia* Baig,
119   Wagner, Ananjeva & Böhme, 2012, *Stellagama* Baig, Wagner, Ananjeva & Böhme, 2012 and

120 *Trapelus* Cuvier, 1817 (Supplementary Tables S1 and S2). For alcohol-preserved voucher

121 specimens, muscle tissue was removed and preserved in 96% ethanol and stored subsequently at

122 -35°C; three tissue samples were obtained from the dried skin of voucher specimens.

DNA extraction, PCR conditions and sequencing

124 Muscle and skin tissues were digested with Proteinase K and total genomic DNA was

125 extracted using a standard phenol-chloroform extraction protocol followed with ethanol

126 precipitation of DNA (Sambrook *et al.* 1989). Our analyses used the mitochondrial DNA dataset

127 of Solovyeva *et al.* (2014), which included the following four mtDNA gene fragments: 654 bp of

128 *COI* (cytochrome oxidase subunit I), 1053 bp of *ND2* (NADH-dehydrogenase subunit II), 705 bp

129 of *ND4* (NADH-dehydrogenase subunit IV) and 297 bp of *Cytb* (cytochrome *b*). The total length

130 of the concatenated mtDNA genes was 2703 bp (Supplementary Table S3). We also amplified

131 exons of four nuclear DNA genes as follows: 1455 bp of *RAG-1* (recombination activating gene),

132 675 bp of *BDNF* (brain derived neurotrophic factor), 1182 bp of *AKAP9* (A-kinase anchor

133 protein 9) and 876 bp of *NKTR* (natural killer-tumor recognition). The total length of these data

134 was 4188 bp (Supplementary Table S3).

135 Primer pairs for PCR were taken from the literature (mtDNA: Ivanova *et al.* 2006; Wang

136 & Fu 2004; Macey *et al.* 2000; Arevalo *et al.* 1994; Pang *et al.* 2003; nuDNA: Shoo *et al.* 2008;

137 Townsend *et al.* 2008; Townsend *et al.* 2011) or designed by us (Supplementary Table S4). PCR

138 amplifications were performed in a reaction volume of 20 µl containing ca. 100 ng of template

139 DNA, 0.3 pM/µl of each PCR primer, 1xTaq-buffer containing 25mM $MgCl_2$ (Silex, Moscow

140 Russia), 0.2 mM dNTPs, and 1 unit of Taq-polymerase (Silex, Moscow Russia; 5 units/µl).

141 Protocols for PCR amplification were provided in the Supplementary Text File 2. PCR products

142 were purified with alcohol precipitation and a PCR purification kit (Isogen, Moscow, Russia).

143 Purified products were sequenced with both forward and reverse primers using ABI PRISM®

144 BigDye™ Terminator v.3.1 reagents and an Applied Biosystems 3730 DNA Analyzer (Applied

145 Biosystems, Carlsbad, CA, USA). All sequencing followed the manufacturer's protocols as

146 given in the Engelgart`s IMB RAN (Moscow, Russia). All unique sequences were deposited in

147 GenBank (Supplementary Tables S1 and S2).

Taxa selection and molecular data

149 We added six sequences of *Phrynocephalus* available in GenBank to the final alignments

150 (Supplementary Table S2). Thirty-seven agamid species were selected as outgroup taxa for

151 phylogenetic inference and time-tree calibration. These included the following Near Eastern and

152 Middle Asian genera closely related to *Phrynocephalus* (Agaminae: *Paralaudakia*, *Laudakia*

153 Gray, 1845, *Trapelus*, *Stellagama*) as well as more distant Southeast Asian agamids (Draconinae:

154 *Acanthosaura* Gray, 1831, *Draco* Linnaeus, 1758, *Calotes* Daudin, 1802; Leiolepidinae:

155 *Leiolepis* Cuvier, 1829) and Australian taxa (Amphibolurinae: *Moloch* Gray, 1841, *Pogona* Storr,

156 1982, *Chlamydosaurus* Gray, 1825). The most distant outgroup taxa also included

157 representatives of Chamaeleonidae, Phrynosauridae, Dactyloidae, Iguanidae, Corytophanidae,

158 Tropiduridae, Polychrotidae, Leiocephalidae, Lacertidae, Opluridae, Crotaphytidae, including

159 representative taxa of the following agamid genera: *Stellagama*, *Trapelus*, *Paralaudakia* and

160 *Agama* for both nuclear and mtDNA dataset, and additionally representative taxa of the genera

161 *Xenagama* Boulenger, 1895, *Laudakia*, *Bufoniceps* Arnold, 1992, *Pseudotrapelus* Fitzinger,

162 1843 and *Calotes* for the mtDNA dataset. Details on taxonomy, GenBank accession numbers and

163 associated references were summarized in Supplementary Tables S1 and S2.

Phylogenetic inference

165 Sequences were first aligned using the Clustal W algorithm (Thompson *et al.* 1994) in

166 BioEdit Sequence Alignment Editor 7.1.3.0 (Hall 1999), with default parameters. Subsequently,

167 the alignment was checked and manually revised if necessary using Seqman 5.06 (Burland 1999).

168 Genetic distances were calculated using MEGA 6.1 (Tamura *et al.* 2013).

169 Phylogenetic tree reconstructions were performed with the following data sets: (1) each

170 nuclear gene separately; (2) all nuclear genes concatenated; (3) all nuclear genes combined in a

171 species tree estimation; (4) a concatenation of four mitochondrial genes as in Solovyeva *et al.*

172 2014 but with the addition of *P. rossikowi* Nikolsky, 1898. To test whether the inclusion of

173 distant outgroups can introduce any bias into results of tree inference, the nuclear and

174 mitochondrial concatenations were put through an additional set of reconstructions omitting all

175 non-agamid and non-agamine taxa, respectively. The optimum partitioning schemes for nuclear

176 and mitochondrial alignments were identified with PartitionFinder (Lanfear *et al.* 2012) using

177 greedy search algorithm under the AICc criterion.

178 Phylogenetic trees were reconstructed under the maximum likelihood (ML), maximum

179 parsimony (MP) and Bayesian inference criteria. The ML trees were generated in Treefinder

180 v.March 2011 (Jobb 2011). For each subset, the best fitting substitution model was selected

181 using the Bayesian Information Criterion in Treefinder. Nodal support was assessed by 1000

182 bootstrap replications (BSP) and expected likelihood weights (ELW). The unweighted MP
183 analyses were conducted in PAUP* v4.0b10 (Swofford 2002) with 1000 bootstrap replications.
184 Bayesian inference (BI) was performed in MrBayes v3.1.2 (Ronquist & Huelsenbeck 2003) with
185 two simultaneous runs, each with four chains, for 200 million generations. We checked the
186 convergence of the runs and that the effective sample sizes (ESS) were all above 200 by
187 exploring the likelihood plots using TRACER v1.5 (Rambaut & Drummond 2007). The initial 10%
188 of trees were discarded as burn-in. Confidence in tree topology was assessed by posterior
189 probability (BPP) (Huelsenbeck & Ronquist 2001).

190   Species-tree estimation was performed in *BEAST (Heled & Drummond 2010) using the
191 four independent nuclear loci. Prior to the analysis, the molecular clock assumption was tested
192 separately for each exon by hierarchical likelihood ratio tests using PAML v4.7 (Yang 2007).
193 Following the results of these tests, we used a strict clock model for *BDNF* and uncorrelated
194 lognormal relaxed clock models for the other three loci. No calibration information was utilized;
195 the clock rate for *BDNF* was set to one. We used the same models and partitioning scheme as in
196 the ML analysis. A Yule prior for the species-tree shape and the piecewise constant population
197 size model were assumed. Default priors were used for all other parameters. Two runs of 500
198 million generations were conducted in BEAST v1.8.0 (Drummond *et al.* 2012). Parameter
199 convergence was assessed in Tracer; the first 10% of generations were discarded as the burn-in.
200 TreeAnnotator v1.8.0 (part of the BEAST package) was used to generate the maximum clade
201 credibility tree.

202   Partition homogeneity test (Farris *et al.* 1994; Farris *et al.*1995) as implemented in
203 PAUP* v4.0b10 (Swofford 2002) was used to ensure the absence of significant conflict among
204 the four nuclear datasets (p-value = 0.071). We a priori regarded tree nodes with BSP values 75%
205 or greater and BPP values over 0.95 as sufficiently resolved (Felsenstein 2004; Huelsenbeck &
206 Hillis 1993). BSP values between 75% and 50% (BPP between 0.95 and 0.90) were regarded as
207 tendencies and below 50% (BPP below 0.90) were considered to be not well-supported.

208 **Congruence between nuclear and matrilineal genealogy**

209   We tested if the mitochondrial genealogy of Solovyeva *et al.* (2014) was compatible with
210 our nuDNA phylogeny to eliminate the possibility of mito-nuclear discordance and an
211 introgressed mitogenome. ML trees with unconstrained and alternative constrained topologies
212 were generated for the mitochondrial and nuclear datasets by using Treefinder v.March 2011.

213 Treefinder was also used to calculate site-wise log-likelihoods and to perform the approximately

214 unbiased tree-selection test (AU; Shimodaira 2002). Significant discordance would have

215 precluded a total evidence approach that evaluated together the mtDNA and nuDNA datasets

216 because we wanted to differentiate between the initial cladogenic event(s) and the timing of

217 interspecific hybridization(s), if present.

Divergence time estimates

219 The mtDNA dataset of Solovyeva *et al.* (2014) and our nuDNA concatenation were used

220 to define divergence times in BEAST v1.8.0 (Drummond *et al.* 2012). Site and clock models

221 were set as in the species tree reconstruction. Analyses were run for 100 million of generations

222 and the Yule model was set as the tree prior. Because no reliable paleontological data have been

223 reported for *Phrynocephalus,* we used ten fossils from non-Agamid outgroup taxa and outgroup

224 Agamidae as calibration points (see Supplementary Table S5, Supplementary Fig. S1).

Area delimitation and biogeographic reconstruction

226 We used the ML of Lagrange (Ree *et al.* 2005; Ree & Smith 2008) to reconstruct the

227 biogeographic history of *Phrynocephalus*. Transitions between discrete states (ranges) along tree

228 branches were modeled as a function of time, thus enabling ML estimation of the ancestral states

229 at cladogenic events. Lagrange found the most likely ancestral areas at a node, the split of the

230 areas in the two descendant lineages, and calculated the probabilities of these most likely areas at

231 each node (Ree & Smith 2008). We defined seven regions for the analyses: Kazakhstan, North

232 Caspian and Ciscaucasian deserts (KZ), Central Asia (CA), Minor Asia and Transcaucasia (MI),

233 Tibet (TI), Turan (TU), Middle East (ME), and Near East and Arabia (AR) (for details on

234 biogeographic regions definition and references see Supplementary Text File 3). The maximum

235 number of regions included in one area was limited to two. We set two periods of time: before 10

236 Ma and after 10 Ma. This date echoed the considerable uplifting of the Pamir, Tianshan and

237 Karakoram mountains. (Abdrakhmatov *et al.* 1996). The matrices of the modern distribution

238 areas were given in Supplementary Table S6.

239 We reconstructed ancestral substrate niche evolution in *Phrynocephalus* under the

240 maximum parsimony criterion using MPRsets command in PAUP* v4.0b10 (Swofford 2002)

241 based on nuDNA topology with outgroup taxa included or excluded from the analysis.

242 Polytomies in the nuDNA-based tree were resolved in accordance with the mtDNA topology. To

243 account for topological uncertainty, the analysis was repeated based on a tree sample (180) from

244 the posterior distribution produced by BEAST. Substrate niche was coded using six character
245 states: (1) loose sand dunes; (2) fixed sands mixed with clay or gravel; (3) gravel and stone
246 deserts; (4) clay soils and salines; (5) clay soils mixed with gravel; and (6) large rocks and cliffs.
247 Transitions between states were formalized using step-matrix (Supplementary Table S7).

248 To examine the evolution of body size in Agaminae, we used weighted squared-change
249 parsimony (Maddison 1991) as implemented in Mesquite v3.31 (Maddison & Maddison 2017).
250 We tested maximum SVL of taxa reported in literature or based on examination of voucher
251 specimens. Maximum SVLs for each taxon were provided in Supplementary Table S6.

252

Results

Taxon sampling, data collection and sequence characteristics

255 The complete, aligned matrix contained 38 samples of *Phrynocephalus* for mtDNA and
256 39 samples for nuDNA, representing 33 of the ca. 40 currently recognized species (Barabanov &
257 Ananjeva 2007; Uetz & Hosek 2016). The concatenated aligned mtDNA dataset encompassed
258 2703 bp and the nuDNA dataset 1488 bp. Information on the length of the fragments and
259 variability were given in Supplementary Table S3. Uncorrected mtDNA genetic distances within
260 *Phrynocephalus* were given in Table 1 (below diagonal).

Phylogenetic inference from mtDNA

262 Analyses of the mtDNA data resulted in the majority of nodes receiving high BSP and
263 BPP support. Topological patterns were in general congruent across analyses and the results of
264 Solovyeva *et al.* (2014). The ML tree is shown in Fig. 2. The result appeared to be insensitive to
265 exclusion/inclusion of distant non-agamid and non-agamine outgroups (see Supplementary Figs.
266 S2–S3).

267 *Phrynocephalus* was unambiguously monophyletic in all analyses (Fig. 2). Several nodes
268 in the mitochondrial tree appeared insufficiently resolved. Nevertheless all species of
269 *Phrynocephalus* were consistently assigned to one of the ten strongly supported matrilines (for
270 their distribution see Supplementary Fig. S4):

271 (1) Subgenus *Microphynocephalus*, joining the small-sized, sand-dwelling *Phrynocephalus*
272   from Middle Asia and the Middle East (Fig. 2; lineage A).

273   (2) Subgenus *Phrynosaurus* represented by *P. scutellatus* from Iranian Plateau (Fig. 2,

274   lineage B).

275   (3) Near and Middle East *Phrynocephalus*: *P. arabicus* Anderson, 1894 and *P. maculatus*

276   Anderson, 1872 (Fig. 2; lineage C), with the latter species being paraphyletic with respect

277   to the former.

278   (4) Subgenus *Megalochilus* Eichwald, 1831, including the large-sized, sand-dwelling *P.*

279   *mystaceus* (Pallas, 1776) from Middle Asia (Fig. 2, lineage D).

280   (5) Subgenus *Oreosaura* joining viviparous Tibetan species (Fig. 2, lineage E).

281   (6) Middle Asian sun-watchers encompassing *P. helioscopus* and allied taxa (Fig. 2, lineage

282   F; *helioscopus*-group).

283   (7) Southern Middle Asian (Turan) *P. raddei* (Boettger, 1889), *P. ocellatus*, *P. rossikowi* and

284   *P. strauchi* Nikolsky, 1899 (Fig. 2, lineage G; *raddei*-group). *P. rossikowi* was omitted in

285   the earlier mtDNA study of Solovyeva et al. (2014); our data strongly support its

286   placement within the *P. raddei* species group.

287   (8) Tibetan oviparous *P. axillaris* Blanford, 1875 (Fig. 2, lineage H).

288   (9) *P. versicolor* species complex, inhabiting northern plains of Central Asia (Fig. 2, lineage

289   I; *versicolor*-group). The *versicolor*-group had two sublineages: *P. hispidus* Bedriaga,

290   1909 from Mongolian Dzungaria and *Phrynocephalus* sp. 1 from Gansu; and *P.*

291   *przewalskii* Strauch, 1876 + *P. frontalis* Strauch, 1876 + *P. versicolor* from central China

292   and Mongolia joined with *P. kulagini* Bedriaga, 1909 from Tuva Republic (Russia).

293   (10)   *P. guttatus* species complex, widespread in plains of Kazakhstan and northern

294   Caspian region (Fig. 2, lineage J; *guttatus*-group). Within the *guttatus*-group, *P. guttatus*,

295   *P. alpherakii* Bedriaga, 1905 and *P. moltschanovi* Nikolsky, 1913 clustered together.

296 **Phylogenetic inference from nuDNA and Mito-nuclear discordance**

297   ML, MP and BI analyses of the concatenated nuclear DNA dataset resulted in highly

298 congruent trees (Fig. 3). Exclusion of non-agamid taxa did not change the topology significantly

299 (Supplementary Fig. S5). Phylogenetic trees resulted from separate analyses of individual genes

300 were shown in Supplementary Figs. S6–S9; values of AU-tests for nuDNA genes compatibility

301 were given in Supplementary Table S8. The topology of the *BEAST species-tree for

302 *Phrynocephalus* and the levels of nodal support (Fig. 4) coincided with the concatenated nuDNA

303   dataset tree (Fig. 3) and were in good correspondence with the topologies from three of the four

304   nuDNA genes (*NKTR*, *RAG-1* and *AKAP9*).

305   Monophyly of *Phrynocephalus* received high support as did several species-groups:

306   *Microphrynocephalus* (Fig. 3, lineage A: 99/100/1), Arabian species-group (Fig. 3, lineage C:

307   100/100/1), *Megalochilus* (Fig. 3, lineage D: 100/100/1), *Oreosaura* (Fig. 3, lineage E:

308   100/100/1) and *P. raddei* species-group (Fig. 3, lineage G: 95/84/1). The *P. heliosopus*-group

309   obtained low support (Fig. 3, lineage F: -/-/0.89), but high support in the species-tree

310   (Supplementary Fig. S4). Monophyly of the clade containing the *P. guttatus*- and *P. versicolor*-

311   groups was highly supported (Fig. 3, lineages I, J: 100/99/1), but interrelationships within this

312   clade remained unresolved. The *P. versicolor*-group was paraphyletic with respect to the *P.

313   guttatus*-group, though with some support only from ELW (Fig. 3: 90/-/-).

314   The nuDNA phylogeny of *Phrynocephalus* conflicted significantly (P < 0.05; AU) from

315   the matrilineal genealogy. The nuDNA topology depicted three main clades (Fig. 3): (1)

316   *Microphrynocephalus*, *P. scutellatus*, Arabian species-group and *Megalochilus* (clades A−D;

317   99/96/1); (2) *Oreosaura* (Clade E; 100/100/1); and (3) all other *Phrynocephalus* (clades F−J;

318   100/99/1). Most notably, the placements of *Megalochilus* and *Oreosaura* differed in important

319   ways. Matrilineally, *Oreosaura* and *Megalochilus* aligned with Middle and Central Asian "core

320   *Phrynocephalus*" with strong support (99/88/1.0). In contrast, the nuDNA biparental phylogeny

321   united *Megalochilus* with Arabian and Iranian species (75/90/0.99), including the *P. arabicus*-

322   group, *P. scutellatus* and *Microphrynocephalus* with *Oreosaura* forming a sister-group to clades

323   A−D. Other notable conflicts also occurred. The nuclear phylogeny did not depict a shared

324   heritage for *P. scutellatus* and the Arabian species-group (Fig. 3), as did the mtDNA genealogy,

325   but rather *P. scutellatus* (Clade B) was the sister-lineage of *Microphrynocephalus* (Fig. 2). The

326   phylogenetic position of *P. strauchi* was contentious; analyses of the nuDNA dataset did not

327   group it with the mtDNA *raddei*-group. Similarly, the phylogeny placed *P. axillaris* as a sister-

328   lineage of the *P. guttatus−versicolor*-group (Figs. 3, 4, Supplementary Fig. S5; 95/91/1), but its

329   matrilineal relationships were unresolved (Fig. 2).

330   We performed additional AU tree-selection test to test for significant differences between

331   matrilineal genealogy and the nuclear phylogeny, including whether one or both datasets rejected

332   alternative placements of particular clades. The test evaluated the conflicting positions of *P.

333   mystaceus*, *P. strauchi*, *P. scutellatus*, *Oreosaura*, the basal position of Arabian species and

334   Arabian species + *Microphrynocephalus*. The matrilineal genealogy was forced to the nuclear

335   dataset and vice versa. AU indexes for the basal position of Arabian species or Arabian species +

336   *P. scutellatus* in the matrilineal genealogy were not statistically rejected by nuclear markers (p =

337   0.217, p = 0.277, respectively). The alternative nuclear hypotheses for the clades A–E and D–H

338   were not rejected by mitochondrial data. The matrilineal position of *P. mystaceus* within the

339   lineage (*Helioscopus* + *P. axillaris* + *P. mystaceus*) was rejected by nuclear markers (p = 0.000),

340   and vice versa mitochondrial markers rejected the nuDNA resolution of *P. mystaceus* + Arabian

341   species + *Microphrynocephalus* + *P. scutellatus* (p = 0.000). The AU test for *P. strauchi*

342   occurring within the *raddei*-lineage was not rejected statistically by nuclear data (p = 0.752) and

343   the mitochondrial data did not reject the nuDNA resolution of *P. strauchi* + *helioscopus*-group (p

344   = 0.857). Existence of the matriline *Oreosaura* + "*guttatus*" + "*versicolor*" was rejected

345   according to nuclear data (p = 0.000) and vice versa the mitochondrial dataset rejected position

346   of *Oreosaura* within A–E (p = 0.000). Finally, we tested topologies of trees based on each

347   nuclear marker against final topology. The *BDNF* dataset rejected the topology. In contrast,

348   original *RAG-1* topology was rejected. P-values of the AU-tests of alternative topologies were

349   summarized in Supplementary Table S9.

350   **Divergence times and rates of change**

351   Chronograms from mtDNA and nuDNA data were presented in Supplementary Figs. S10

352   and S11, respectively. Timing of the internal nodes was summarized in detail in Supplementary

353   Table S10. Estimated node-ages and the 95% highest posterior density (95% HPD) for the main

354   nodes were detailed in Supplementary Table S10. The mtDNA dataset provided older estimates

355   of ages as compared to nuDNA. All analyses proposed that the ancestor of *Phrynocephalus*

356   originated between the end of Oligocene and beginning of the Miocene (mtDNA: 33.2 Ma (26.4–

357   39.7); nuDNA: 26.9 Ma (22.6–31.7)) and the basal radiation dated to the Middle Miocene

358   (mtDNA: 19.3 Ma (14.9–23.5); nuDNA 14.8 Ma (12.0–17.5)).

359   LTT plots gave a graphical representation of lineage-accumulation (Supplementary Fig.

360   S12). The mtDNA (Fig. S12A) and nuDNA (Fig. S12B) plots had similar shapes that were best

361   described as being anti-sigmoidal characterized by three periods of constant rate. The first rate

362   constant was separated from the second by a plateau and occurred before 14 Ma for mtDNA and

363   before 11 Ma for nuDNA and the second plateau occurred after these dates. The third period

364   started after 5 Ma, followed by a slight rate-shift in both plots.

365 **Ancestral area, substrate niche and body size evolution modeling**

366   The ancestral areas and biogeographic processes (vicariance, dispersal and colonization
367 routes) reconstructed from nuDNA data were shown in Fig. 5. The most likely biogeographic
368 scenario suggested that the Middle East plus the Turan area (ME-TU) was the most probable
369 ancestral area for *Phrynocephalus*, thus supporting the hypothesis of a southern origin.
370 Paleogeography of central Eurasia in Miocene–Pliocene was shown in Fig. 6.

371   Results of habitat evolution modelling for *Phrynocephalus* were given in Fig. 7. All
372 simulations of the possible evolution of substrate niches in *Phrynocephalus* suggested that the
373 most likely substrate type for the ancestor consisted of soft substrate, i.e. loose sands with non-
374 differentiated proluvial sediments, such as clay or gravel.

375   Results of ancestral state reconstructions of maximum SVL evolution for each taxon were
376 shown in Fig. 8. Accordingly, the common ancestor of *Phrynocephalus* was likely significantly
377 smaller (size category 87–97 mm) than its sister taxa *Laudakia*, *Stellagama* and *Paralaudakia*
378 (ancestral size category 147–157 mm). Most species of *Phrynocephalus* have been found to be
379 smaller than their common ancestor (size categories 47–77 mm); however, several lineages of
380 *Phrynocephalus* have subsequently increased their body size (*P. maculatus*: 87–97 mm; *P.
381 mystaceus*: 77–127 mm), while further miniaturization was suggested for the *P. interscapularis*-
382 group (37–47 mm).

383

384 ## Discussion

385 ### Phylogenetic relationships of *Phrynocephalus*

386   Supplementary Text File 1 provides a brief review on history of phylogenetic studies of
387 the genus *Phrynocephalus*.

388   **Phylogenetic placement of *Phrynocephalus*.** Our results are in accordance with previous
389 studies on the higher phylogenetic relationships within the subfamily Agaminae (Macey *et al.*
390 2000; Guo *et al.* 2007; Melville *et al.* 2009) (Figs. 2 and 3). Sand-dwelling *Bufoniceps
391 laungwalaensis* (Sharma 1978) from the Thar Desert of India, which was originally described as
392 a species of *Phrynocephalus* (Sharma 1978), is the sister-lineage of the Middle Eastern–Middle
393 Asian genus *Trapelus*; this corresponds with results of Macey *et al.* (2006) and Melville *et al.*
394 (2009). The clade (*Phrynocephalus* + *Laudakia* s.l.) is poorly resolved; the old age of this

395 radiation, which we estimate as early to mid-Oligocene (Supplementary Figs. S10, S11), likely

396 complicates phylogenetic resolution. Future genome-scale studies are likely to recover these

397 relationships. Regardless, the monophyly of *Phrynocephalus* (excluding *Bufoniceps*

398 *laungwalaensis*) is unambiguous in all analyses.

399 **Phylogenetic relationships within *Phrynocephalus*.** Analyses of nuclear gene exons

400 (Fig. 3) resolve the phylogenetic relationships for most of the species-groups revealed by the

401 matrilineal genealogy (Fig. 2), including the following: *P. interscapularis*-group (subgenus

402 *Microphrynocephalus*; lineage A on mtDNA-genealogy), subgenus *Oreosaura* (lineage E), *P.*

403 *guttatus*- and *P. versicolor*-groups (lineages J and I, respectively), *P. mystaceus* (subgenus

404 *Megalochilus*; lineage D), *P. helioscopus* (lineage F) and *P. arabicus–P. maculatus* (lineage C).

405 The *P. guttatus*- and *P. versicolor*-matrilines are sister-groups, although concatenated analyses of

406 nuDNA data nest the former within the latter (Fig. 3) and the species-tree suggests sister-group

407 relationships (Fig. 4). These are the youngest associations within *Phrynocephalus*. MtDNA

408 analyses resolve close relationships between the *P. helioscopus*-group and *P. axillaris*, but

409 analyses of nuDNA data resolve *P. helioscopus*-lineage + *P. ocellatus*-lineage with strong

410 support and place *P. axillaris* as the sister clade to the *P. guttatus* + *P. versicolor* lineages.

411 Overall, the nuDNA phylogenetic trees are generally better resolved and show higher

412 nodal support values than the mtDNA trees. The nuDNA phylogeny also shows higher

413 congruence with traditional systematics of the genus. Owing to biparental inheritance, we prefer

414 the nuDNA topology as the phylogeny of the genus *Phrynocephalus* (Fig. 3), which coincides

415 well with the species-tree (Fig. 4). Further, the matrilineal genealogy appears to resolve the

416 introgression of mitogenomes via interspecific hybridization (below). In general,

417 *Phrynocephalus* has three main clades, but the relationships among them are not well-supported.

418 Clade I (Fig. 4) contains the *P. interscapularis*-group (subgenus *Microphrynocephalus*),

419 *P. arabicus–P. maculatus*-group, *P. scutellatus* and *P. mystaceus* (subgenus *Megalochilus*). The

420 phylogenetic relationships between these four groups are essentially unresolved. This groups

421 includes oviparous species inhabiting Arabia, Near to Middle East and Middle Asia. Many of

422 them associate with sand dunes. Monophyly of the *P. arabicus–maculatus* group and

423 *Microphrynocephalus* (*P. interscapularis–P. ornatus* Boulenger, 1887 -group) has strong support.

424 Clade II (Fig. 4) includes viviparous species inhabiting high elevations of the QTP

425 (subgenus *Oreosaura*). Phylogenetic relationships within this group remain unresolved with the

426 exception of a sister-species relationship between *P. theobaldi* Blyth, 1863 and *P. forsythii*

427 Anderson, 1872. In the concatenated analysis of nuDNA exons (Fig. 3), monophyly of the group

428 that includes Clade I and Clade II receives strong support (75/90/0.99), although this node does

429 not receive high support in the species-tree analysis (Fig. 4).

430   Clade III (Fig. 4), the "core" *Phrynocephalus*, contains all remaining taxa of the genus

431 and consists of oviparous lowland species inhabiting arid areas of Central and Middle Asia and

432 the Middle East. It includes two strongly supported groups: *P. helioscopus–P. raddei* and *P.*

433 *guttatus–P. versicolor*. Monophyly of the *P. helioscopus* species complex and the *P. ocellatus–P.*

434 *raddei*-group receives strong support. The phylogenetic position of *P. strauchi* remains

435 unresolved, while *P. axillaris* appears as the sister-taxon of the *P. guttatus– P. versicolor*-group,

436 which coincides with morphology; *P. axillaris* and members of the *P. guttatus–P. versicolor*

437 species complexes share a number of morphological similarities, including having bright axillary

438 spots possibly used in signaling communication (Fig. 3).

439   Our phylogeny has better resolution and wider taxon sampling than previously published

440 mtDNA-based genealogies (Pang *et al.* 2003; Guo *et al.* 2007; Melville *et al.* 2009; Solovyeva *et*

441 *al.* 2014) and the nuDNA-based phylogeny (1200 bp fragment of *RAG-1*) of Melville *et al.*

442 (2009). Our tree also differs from the morphological phylogeny of Arnold (1999), in which the

443 Tibetan viviparous *Oreosaura* appear to be deeply nested within the core clade of

444 *Phrynocephalus* and nests with the *P. helioscopus*-group, while *P. mystaceus*, *P. arabicus*, *P.*

445 *longicaudatus* Haas, 1957 (as *P. maculatus*) and *Microphrynocephalus* occupy the basal position

446 in the *Phrynocephalus* radiation. The potential explanation of these differences may be

447 connected with habitat preferences; adaptation to types of substrate may drive convergent

448 changes and morphology. Both Tibetan viviparous *Oreosaura* and *P. helioscopus*-group

449 members occur mostly on solid (rocky or clay) substrates and are superficially similar in external

450 morphology, sharing robust body habitus, shortened tail and other features. At the same time,

451 sand-dwelling *Microphrynocephalus*, *P. mystaceus* and *P. arabicus* and *Bufoniceps* share such

452 characters as presence of enlarged scale fringes on toes, enlarged or keeled scales on throat,

453 eyelids or jaws, flattened body and tail, which are considered to be adaptive for life on large

454 wind-blown sand dunes. Arnold (1999) rooted his tree with *Trapelus* and *Bufoniceps*. However,

455 convergent similarity between send-dwelling *Phrynocephalus* and *Bufoniceps* potentially could

456 lead to the basal position of *P. mystaceus*.

Mito-nuclear discordance due to ancient hybridization. The main difference between mt- and nuDNA trees is the positions of *P. mystaceus*: the nuDNA-based topology strongly suggests that *P. mystaceus* as a sister-group with respect to the Middle-Eastern *P. interscapularis*-group (*Microphrynocephalus*), *P. scutellatus* and the Arabian *P. arabicus–P. maculatus*-group (Fig. 3). In contrast, the mtDNA genealogy unambiguously places *P. mystaceus* within core *Phrynocephalus* with *P. axillaris* being a possible sister-lineage (Fig. 2). The AU tests either rejects or do not provide statistical support for genomic compatibility (except as noted above; Supplementary Table S8). Mitochondrial and nuclear genetic markers have yielded many conflicting geographic patterns (reviewed by Toes & Brelsford 2012). Examples of mito-nuclear discordance in reptiles remain limited (McGuire *et al.* 2007; Zarza *et al.* 2011; Pedall *et al.* 2010; Renoult *et al.* 2009; Leache & Cole 2007; Ng & Glor 2011; Nguyen *et al.* 2017), perhaps because the discrepancy is rarely tested. Different mechanisms and rates of evolution for mt- and nuDNA may account for some observed topologic discrepancies. Fisher-Reid and Wiens (2011) evaluated 14 vertebrate clades for which both mtDNA and nuDNA data exist and reported that 30–60% of the nodes differed between trees from the two genomes. The results of our AU-tests suggest that topological differences between mtDNA and nuDNA hypotheses can be statistically significant. Thus, our analyses suggest that the combining of data from the two genomes should be avoided or done with caution without first testing for compatibility. Equally important, analyses based on combined datasets may hide biogeographic histories of studied taxa due to gene sorting, genetic recombination and gene flow of nuDNA (Nguyen *et al.* 2017).

Several processes, including incomplete lineage sorting or introgressive hybridization, may best explain mito-nuclear discordance (Toes & Brelsford 2012). The deep divergence between *P. mystaceus* and core *Phrynocephalus*, as well as the unique morphology of this large-sized species differing from any other congener (Fig. 3), renders incomplete lineage sorting an unlikely scenario (McGuire *et al.* 2007). Thus, in case of *P. mystaceus*, an ancient introgression of mitochondrial genome due to interspecific hybridization best explains the discordance. According to mtDNA time-tree (Supplementary Fig. S10) divergence between mitochondrial genomes of ancestral *P. mystaceus* and *P. axillaris* took place in late Miocene (around 10.4 Ma), whereas the basal differentiation of *Phrynocephalus* is estimated as the middle Miocene (around 14.8 Ma; Supplementary Fig. S11) according to nuDNA data. Hence, the possible hybridization between *P. mystaceus* and *P. axillaris* ancestors occurred approximately 5 Ma after speciation,

488   and this roughly corresponds to the level of divergence within the present-day *P. guttatus*–*P.*
489   *versicolor* species complexes. This timing makes interspecific hybridization possible. Further,
490   male-biased dispersal favors mitochondrial genome introgression (Toes & Brelsford 2012) and
491   *Phrynocephalus* appears to have male-mediated gene flow. Discordant breaks in mtDNA and
492   nuDNA markers occur in at least for four species: *P. vlangalii*–*P. putjatai* Bedriaga, 1909-groups
493   (Noble *et al.* 2010; Qi *et al.* 2013), and in the *P. przewalskii*–*P. frontalis*-groups (Uruquhart *et al.*
494   2009). Other lineages may have the same pattern. *Phrynocephalus mystaceus* is the largest
495   species of the genus and it shows adaptations typical of a psammophilous lifestyle including
496   triangular scales forming fringes on toes, ridged subdigital lamellae, distinctly flattened body and
497   tail, and a pair of unique cutaneous flaps at mouth corners with numerous spiny scales along flap
498   edges. Similar spiny scales can occur in mouth corners of miniaturized psammophilous members
499   of the *P. interscapularis*-group and *P. euptilopus* Alcock et Finn, "1896" 1897. These species are
500   similar to *P. mystaceus* and occur in the Middle East and Middle Asia. Thus, our nuDNA
501   phylogenetic hypothesis corresponds with life history, biogeographic and morphological
502   similarities between *P. mystaceus* and smaller psammophilous taxa of *Phrynocephalus*.

Taxonomic implications

504   The results of our phylogenetic analyses require some taxonomic changes within
505   *Phrynocephalus*. These include recommendations on genus- and species-level taxonomy.

506   **Generic taxonomy of *Phrynocephalus*.** The significant morphological diversity of
507   *Phrynocephalus* has been reflected in their generic taxonomy. First, Eichwald (1831) proposed
508   the new name *Megalochilus* for the largest species of the genus, *P. mystaceus*. Ananjeva (1987)
509   recognized the genus, but this was not accepted by subsequent researchers (e.g. Zhao & Adler
510   1993; Dunayev 1996; Arnold 1999). Sharma (1978) described *P. laungwalaensis* from Rajasthan
511   (India), but Arnold (1992) removed it from *Phrynocephalus* and reassigned it to monotypic
512   *Bufoniceps*, which he treated as a sister-clade of *Phrynocephalus*, Subsequent molecular analyses
513   supported this arrangement (Macey *et al.* 2006; Melville *et al.* 2009). Based on the phylogenetic
514   analysis by Pang *et al.* (2003), Barabanov and Ananjeva (2007) suggested recognizing the
515   Tibetan viviparous species-group as subgenus *Oreosaura*. Because the phylogenetic
516   relationships within oviparous species remained largely unknown, this subgeneric taxonomy was
517   not largely accepted. Solovyeva *et al.* (2014) analyzed four mtDNA gene fragments and the
518   morphological data of Arnold (1999) and suggested that small-bodied sand-dwelling

519 *Phrynocephalus*, including the *P. interscapularis*-group and *P. ornatus*, constituted a
520 morphologically and phylogenetically distinct group; they erected new subgenus
521 *Microphrynocephalus* for it. However, our nuDNA-based phylogeny requires reconsideration of
522 this arrangement.

523   Excluding *Bufoniceps laungwalaensis*, nuDNA, mtDNA (herein) and morphological
524 (Arnold 1999) analyses indicate monophyly of *Phrynocephalus*. Thus, the splitting of
525 *Phrynocephalus* into several genera is inadvisable. Further molecular studies are necessary to
526 test for monophyly of *Laudakia* s.l. and its relationships with respect to *Phrynocephalus*.

527   The recognition of subgenera within *Phrynocephalus* is a matter of taste. The genus has
528 three clearly defined clades that may warrant taxonomic recognition. The largest of these clades,
529 or the "core" *Phrynocephalus* (Clade III, Fig. 4), encompasses the majority of oviparous species
530 and corresponds to the nominative subgenus *Phrynocephalus* s.s. Clade II (Fig. 4) unites
531 viviparous species of the QTP and is well-defined by morphology and life history traits;
532 subgenus *Oreosaura* applies to it. Last, Clade I (Fig. 4) joins a number of species from Arabia,
533 Middle East and Middle Asia that have plesiomorphic character states (Arnold (1999), including
534 the *P. arabicus–P. maculatus*-group, *P. interscapularis–P. ornatus*-group, *P. scutellatus* and *P.*
535 *mystaceus*. The *P. interscapularis–P. ornatus*-group, which was erected as subgenus
536 *Microphrynocephalus* Dunayev, Solovyeva, Poyarkov, 2014 (Solovyeva *et al.* 2014) are
537 miniaturized species adapted to life in aeolian sand habitat and they share a number of
538 morphological synapomorphies (Arnold 1999) and geographic coherence. The older name
539 *Phrynosaurus* Fitzinger, 1843 is available. However, the phylogenetic position of its type
540 species—*P. olivieri* Duméril et Bibron, 1837, which is now considered as a junior synonym of *P.*
541 *scutellatus* (Olivier)—within the clade remains unclear. Finally, *P. mystaceus*, to which the name
542 *Megalochilus* Eichwald, 1831, is available, forms a sister-group with respect to all other
543 members of Clade I. This species has a unique morphology and evolutionary history, which
544 likely includes an episode of ancient intraspecific hybridization with introgression of its
545 mitochondrial genome from Clade III species.

546   Two alternative taxonomic decisions are possible: recognizing the whole of Clade I as
547 *Megalochilus*, or splitting it into a number of smaller taxa, including *Megalochilus*,
548 *Phrynosaurus*, *Microphrynocepahlus* and an unnamed taxon for the *P. arabicus–P. maculatus*
549 species group. Our analyses lack samples from a number of Middle Eastern species, which likely

550 fall into Clade I, including *P. ornatus ornatus*, *P. clarkorum* Anderson et Leviton, 1967, *P.*
551 *lutensis* Kamali & Anderson, 2015, *P. luteoguttatus* Boulenger, 1887 and, most importantly,
552 large-sized and psammophilous *P. euptilopus*. Accordingly, we suggest that further taxon
553 sampling and additional nuDNA-markers be evaluated before making subgeneric changes in the
554 interest of maintaining taxonomy stability.

555 **Taxonomic differentiation within species complexes.** Our results indicate that in many cases
556 the currently adopted taxonomy is incomplete and does not reflect the actual biodiversity within
557 *Phrynocephalus*. We briefly review these cases and provide corresponding taxonomic
558 recommendations.

559

560 **Lineage A. *Microphrynocephalus*.** This group of miniaturized species inhabit wind-
561 blown sands of southern Middle Asia (Turan) and Middle East. Our analyses include *P.*
562 *interscapularis*, *P. sogdianus* Chernov, 1948 and *P. ornatus vindumi* Golubev, 1998 only.
563 Although unsampled, *P. ornatus ornatus*, *P. clarkorum*, *P. luteoguttatus*, *P. lutensis* most likely
564 belong to this group based on morphological characters (Arnold 1999; Kamali & Anderson
565 2015). *Phrynocephalus sogdianus* was described from southern-most Tajikistan by Chernov
566 (1948) as a subspecies of *P. interscapularis* (type locality "vicinity of the Pyandzh [= Panj]
567 village"). Later, Sokolovsky (1975) raised it to be a full species. Our locality for *P. sogdianus*,
568 Kurjalakum Sands, occurs approximately 50 km from the type locality and the Vakhsh River
569 Valley separates it from the type locality. Our substantial divergence in mtDNA sequences
570 (uncorrected genetic *p*-distance = 3.9–4.3% for *COI*) coincides with morphological and
571 distributional differences and favors the recognition of *P. sogdianus* as a full species.

572 **Lineage B. *Phrynocephalus scutellatus*.** The phylogenetic position of this small-sized
573 species, which inhabits clay or gravel deserts on the Iranian Plateau, remains unclear within
574 Clade I. The recent molecular study of Rahiamian *et al.* (2015) identified at least four highly
575 divergent matrilines in southern and north-eastern Iran. Thus, *P. scutellatus* might consist of a
576 species complex that requires reconsideration.

577 **Lineage C. Arabian group.** Our analyses include psammophilous *P. arabicus* s.l., which
578 inhabits aeolian sand dunes from the Arabian Peninsula to westernmost Iran, and *P. maculatus*,
579 which occurs on hard substrates and has two presently recognized subspecies: *P. m. maculatus*
580 (Anderson) from the Iranian Plateau and *P. m. longicaudatus* from the Arabian Peninsula. Our

581 sampling lacks *P. golubewii* Shenbrot et Semenov, 1990 from Turkmenistan and *P. sakoi*

582 Melnikov, Melnikova, Nazarov, Al-Johany & Ananjeva, 2015 from Oman. Melnikov *et al.* (2014)

583 revised *P. arabicus* complex, considered *P. nejdensis* Haas, 1957 and *P. macropeltis* Haas, 1957

584 as valid species, and described the population of *P. arabicus* s.l. from western Iran as the new

585 species *P. ahvazicus* Melnikov, Melnikova, Nazarov, Rajabizadeh, Al-Johany, Amr & Ananjeva,

586 2014. However, this taxonomic action was based primarily on small to moderate genetic

587 distances between these forms (*p*-distance 2.7%–6.0%) and differences observed in coloration of

588 living animals. Because Melnikov *et al.* (2014) did not include many morphological and meristic

589 characters that serve to diagnose the species, these data must be taken with caution (Kamali &

590 Anderson 2015). Our sample from western Iran corresponds to *P. ahvazicus* of Melnikov *et al.*

591 (2014). However, we tentatively assign it as *P. arabicus* s.l. pending a further re-assessment of

592 the taxonomy of the *P. arabicus* species complex. Previously, Solovyeva *et al.* (2014) suggested

593 that paraphyly of *P. maculatus* s.l. occurred with respect to *P. arabicus*. Our multilocus nuDNA-

594 based phylogeny agrees with the matrilineal genealogy and indicates that *P. longicaudatus* from

595 the Arabian Peninsula is a sister-taxon of *P. arabicus* (*p*-distance = 8.0% for *COI*). This differs

596 from *P. maculatus* from Iran being reconstructed as a sister-taxon to the clade joining *P.*

597 *arabicus* and *P. longicaudatus*. Based on the principle of monophyly, as well as genetic and

598 distributional differences, we raise *P. longicaudatus* to full species status as *Phrynocephalus*

599 *longicaudatus* (Haas 1957) **comb. et stat. nov.**

600 **Lineage D. *Megalochilus*.** *Phrynocephalus mystaceus* represents a widespread species-

601 complex that inhabits wind-blown sands and large sand dunes from north-eastern Iran to the

602 Turan region, Middle Asia and the Caspian Basin. While intraspecific taxonomy within *P.*

603 *mystaceus* is in a state of flux, we report on two highly divergent lineages within this complex

604 that were firstly revealed by mtDNA sequences (Solovyeva *et al.* 2014; *p*-distance = 6.3–6.5%

605 for *COI*). Nuclear markers also reveal deep divergence between these two lineages, one of which

606 is restricted to East Khorasan Province, Iran (*P. mystaceus* 2) and another occupies the rest of

607 species range in Middle Asia (*P. mystaceus* 1). Thus, the taxonomy of this complex requires

608 further study.

609 **Lineage E. *Oreosaura*.** This clade consists of viviparous highland species inhabiting

610 deserts of the QTP and our analyses evaluate *P. erythrurus*, *P. forsythii*, *P. putjatai*, *P. vlangalii*,

611 and *P. theobaldi* within the complex. The phylogenetic relationships among these species remain

612 essentially unresolved. Pang *et al.* (2003), Jin *et al.* (2008; 2017), Jin & Liu (2010), Noble *et al.*
613 (2010) and Zhang *et al.* (2010) assessed their phylogenetic relationships and biogeography.

614   **Lineage F. *P. helioscopus–P. persicus*-group.** This group, which was until recently
615 considered to be a widespread polytypic species *P. helioscopus* s.l., occurs in the montane
616 deserts from western and northern Iran, Transcaucasia, the Turan Region and Middle Asia to the
617 Caspian Basin in the west and westernmost China and Mongolia in the east. *Phrynocephalus*
618 *helioscopus* has a robust, tuberculate morphology and inhabits mostly hard substrates in clay or
619 clay/gravel deserts. Previous phylogenetic analyses of mtDNA (*COI*) and nuDNA (interSINE-
620 PCR) by Solovyeva *et al.* (2011) indicated the presence of two main clades within this complex:
621 *P. helioscopus* complex (Middle Asia and adjacent territories) and *P. persicus* De Filippi, 1863
622 complex (Iran and Transcaucasia), both of which contained a number of highly divergent
623 lineages. Subsequent analysis of morphological characters resulted in recognizing seven
624 subspecies within *P. helioscopus* and three within *P. persicus* (Solovyeva *et al.* 2012). Our
625 phylogeny does not support monophyly of the *P. helioscopus* + *P. persicus* group (Fig. 2),
626 although the species-tree does (Fig. 4). The *P. helioscopus* complex is a monophyletic unit. Deep
627 divergences in both mtDNA and nuDNA genes occur between *P. saidalievi* Sattorov, 1981 from
628 Ferghana Valley, Uzbekistan and Tajikistan and *P. h. helioscopus* + *P. h. varius* Eichwald, 1831
629 (p = 12.0–12.6% in *COI*). Eremchenko & Panfilov (1999) proposed full species status for *P.*
630 *saidalievi* based on differences in karyotype and our analyses strongly support this arrangement.
631 Based on the principle of monophyly, along with the molecular and morphological analyses of
632 Solovyeva *et al.* (2011; 2012), we also recognize *Phrynocephalus meridionalis* Dunayev,
633 Solovyeva, Poyarkov in Solovyeva, 2012 **comb. et stat. nov.** This species is the sister-taxon of *P.*
634 *saidalievi* and was originally described as a subspecies of *P. helioscopus* from the Surkhandarya
635 Region of southern Tajikistan. The species differs markedly in its mtDNA sequences (p = 10.0–
636 10.6% in *COI*), nuclear markers and morphology (Solovyeva *et al.* 2011; Solovyeva *et al.* 2012).
637 Future studies can address further taxonomic reassignments within the *P. helioscopus* and *P.*
638 *persicus* complexes.

639   **Lineage G. *P. raddei–P. ocellatus* group.** This group contains a number of species that
640 have comparatively small distributions involving gravel or clay-gravel deserts of Turkmenistan,
641 Uzbekistan and eastern Tajikistan. Unfortunately, we were unable to obtain nuDNA sequences
642 from our sample of *P. rossikowi* due to poor quality of the DNA from this sample; however, our

643   mtDNA analysis strongly suggests that *P. rossikowi* is a member of this species group, and this is
644   concordant with morphological similarity and ecology of this species, which prefer solid
645   substrates (salines) (Solovyeva 2017). Until recently, with the exception of *P. rossikowi*, two
646   species were recognized: *P. raddei* Boettger, 1888 (subspecies *P. raddei raddei* Boettger, 1888
647   from Turkmenistan and *P. raddei boettgeri* Bedriaga, 1905 from Uzbekistan) and *P. reticulatus*
648   Eichwald, 1831 (subspecies *P. re. reticulatus* Eichwald, 1831 from Uzbekistan, *P. re. bannikovi*
649   Darevsky, Rustamov et Shammakov, 1976 from Turkmenistan and *P. re. strauchi* from Ferghana
650   Valley in Uzbekistan and Tajikistan; Terentjev & Chernov 1949; Wermuth 1969, Bannikov *et al.*
651   1977; Barabanov & Ananjeva 2007). Barabanov & Ananjeva (2007) considered *P. boettgeri* a
652   junior synonym of *P. raddei*. Golubev (1991) examined the type specimens of *Agama ocellata*
653   Lichtenstein in Eversmann, 1823 and demonstrated that it was the senior synonym of *P.*
654   *reticulatus* Eichwald, 1831, which he considered as a subjective junior synonym of the former.
655   Subsequently, the name *P. ocellatus* (Lichtenstein in Eversmann, 1823) was widely accepted for
656   over 25 years (e.g. Dunayev 1996; Dunayev 2007; Golubev *et al.* 1995; Manilo 2000, 2001;
657   Manilo & Golubev 1993; Szczerbak 1994; Solovyeva *et al.* 2014). Despite that, Barabanov &
658   Ananjeva (2007: 56) proposed to protect the name *P. re. reticulatus* and in doing so violated the
659   principle of priority (ICZN 1999). Herein, we follow Golubev (1991) and use the name *P.*
660   *ocellatus* in order to maintain nomenclatural stability and priority.

661   Our mtDNA analyses suggest monophyly of the *P. raddei boettgeri*–*P. ocellatus* group
662   and suggest that *P. strauchi* is their sister-group. Their relationships within *Phrynocephalus*
663   remain unresolved (Fig. 2). Concatenated (Fig. 3) and species-tree (Fig. 4) analyses of nuclear
664   loci resolve paraphyly within the group. The phylogenetic position of *P. strauchi* is unresolved
665   and *P. raddei boettgeri*–*P. ocellatus* form a well-supported sister-group relationships with *P.*
666   *helioscopus*–*P. persicus* (lineage F). This clearly supports giving full-species status of *P.*
667   *strauchi* as suggested by Dunayev (1995). Our sampling within this group is incomplete because
668   we lack *P. bannikovi* and *P. raddei raddei* from Turkmenistan. Further studies are required to
669   clarify phylogenetic relationships within this group.

670   **Lineage H. *P. axillaris*.** Oviparous *P. axillaris* from sand deserts of Taklimakan and
671   adjacent parts of western China is a highly divergent lineage according to our concatenated (Fig.
672   3) and species-tree (Fig. 4) analyses of nuDNA-markers. It is the sister-taxon of lineages I–J (*P.*
673   *guttatus*–*P. versicolor*-group). These lizards have a slender habitus, share habitat preferences and

674   have bright red to blue axillary spots used in intraspecific communication (Fig. 3). Zhang *et al.*

675   (2010) reported on the phylogeography of this species.

676   **Lineages I–J. *P. guttatus–P. versicolor* group.** Analyses of both mtDNA (Fig. 2) and

677   nuDNA (Figs. 3 and 4) datasets suggest monophyly of the group. They are morphologically

678   diverse oviparous species from lowland deserts of northern Middle and Central Asia. While

679   analyses of the mtDNA data indicate reciprocal monophyly of *P. guttatus* and *P. versicolor*

680   lineages, analyses of nuDNA data nest latter within the former. The *P. guttatus*-group (lineage J)

681   inhabits various types of deserts ranging from sand dunes to gravel deserts. They occur in the

682   Middle Asia from Caspian Basin to the westernmost China. Dunayev (1996; 2009) assessed the

683   taxonomy and distribution of lizards in Kazakhstan. NuDNA sequences fail to resolve

684   relationships within this complex, yet mtDNA markers suggest the presence of three main

685   matrilines: (1) *P. guttatus*, *P. moltschanovi* and *P. alpheraki* from the Caspian and Aral basins

686   and Ili Depression in eastern Kazakhstan; (2) *P. kuschakewitschi* Bedriaga, 1905 and *P. incertus*

687   Bedriaga, 1905 from the Balkhash Lake Basin in eastern Kazakhstan; and (3) *P. melanurus* from

688   the Zaysan Depression in northeastern Kazakhstan and Junggar Depression of northwestern

689   China. Significant differentiation in mtDNA sequences (p=4.0–7.9% for *COI*), morphology and

690   distribution argue for recognizing these forms of *P. guttatus* as full species. However, further

691   research including more variable nuclear DNA-markers is necessary before doing so, especially

692   in the Balkash Lake Basin in Eastern Kazakhstan, which cradles the highest species diversity of

693   this group and where gene flow between species might take place (Solovyeva et al., in prep.).

694   Lineage I comprises the species of *P. versicolor*-group that inhabit lowland deserts of

695   northern Central Asia. Whereas the nuDNA analyses do not resolve relationships within this

696   group, mtDNA results suggest the presence of two matrilines, one containing populations from

697   the Mongolian part of the Junggar Depression (Mongolian Jungaria), previously assigned to *P.*

698   *versicolor hispida* (Orlova *et al.* 2014). Concatenated analysis of nuDNA loci suggest its

699   recognition as the full species *Phrynocephalus hispidus* Bedriaga, 1909 **comb. et stat. nov.** The

700   mtDNA divergence of this lineage from other members of *P. versicolor* group is substantial (p =

701   6.7–7.3%). Our analyses are in concordance the previous results by Gozdzik & Fu (2009) and

702   Urquhart *et al.* (2009) on genetic uniformity of *P. przewalskii* and *P. frontalis*. Despite the

703   presence of two matrilines, the nuDNA markers do not differ between the two and

704   *Phrynocephalus przewalskii* Strauch, 1876 appears to be the senior synonym for this taxon.

705   *Phrynocephalus versicolor* is a wide-ranging species that inhabits the Mongolian and

706   Chinese Gobi Desert as far northwards as the Tuva Republic in southern Siberia (Russia).

707   Traditionally, two subspecies were recognized: *P. v. kulagini* from Tuva and northern Mongolia

708   and *P. v. versicolor* from the rest of species' range. Previous studies (Wang & Fu 2004) did not

709   include samples of *P. v. kulagini*; our analyses strongly indicate paraphyly of *P. versicolor* s.l.

710   with specimens from Tuva being significantly differentiated both in mtDNA ($p = 5.18\%$–5.37%

711   for *COI*), nuDNA genes, and morphology. These results are supported by morphological

712   differentiation (Dunayev 2009), and this requires recognition of the full species *Phrynocephalus*

713   *kulagini* Bedriaga, 1909 **comb. et. stat. nov.**

714 **Implications for morphological and ecological evolution**

715   **Ancestral structural substrate niche.** A debate exists on the ancestral habitat niche of

716   *Phrynocephalus*. Several authors suggested that the common ancestor *Phrynocephalus* was

717   likely adapted to soft, wind-blown sand dunes (Chernov 1948; Whiteman 1978; Arnold 1999),

718   whereas others argued that the group arose in stony or clay deserts with solid ground (Ananjeva

719   & Tuniyev 1992, Golubev 1989). Arnold (1999) provided a morphology-based phylogeny for

720   *Phrynocephalus*, and with *Trapelus* and *Bufoniceps* reconstructed as its sister-taxa. He assumed

721   that this group of genera demonstrated a gradual adaptation to soft substrates, such as loose

722   aeolian sand-dunes.

723   We reconstructed the evolution of the preferred habitat types among all sampled

724   *Phrynocephalus* and Agaminae outgroups using MP (Fig. 7, Supplementary Table S6). Most

725   Agaminae genera climb to some extent (Arnold 1999) as *Agama*, *Pseudotrapelus* and *Laudakia*

726   s.l. exhibit. These taxa are found mostly frequently on large rocks and boulders, and this also

727   occurs for most *Trapelus*, which inhabit sandy or gravel deserts, but eagerly climb bushes and

728   trees. Only three genera—*Xenagama*, *Bufoniceps* and *Phrynocephalus*—are strictly ground-

729   dwelling, and this appears to be the derived condition. Our analysis suggests that two lineages

730   within Agaminae independently adapted to life on soft substrates: the common ancestor of

731   *Trapelus* and *Bufoniceps*, and the ancestor of *Phrynocephalus*.

732   Loose sands with non-differentiated proluvial sediments appear to be the ancestral habitat

733   of *Phrynocephalus*. This initial adaptation could result in evolution of a set of advantageous

734   features typical for this genus, such as (1) skin covering the tympanum, (2) lateral fringes of

735   elongate scales on digits and eyelids, (3) countersunk jaws, (4) flattened body and tail and (5) a

736 characteristic burial behavior by lateral oscillations of the body (Arnold 1999; Dunayev 1996).
737 Further differentiation within *Phrynocephalus* likely led to adaptations of different lineages to
738 contrasting habitat preferences. *Phrynocephalus* of Clade I mostly specialize for life on sandy
739 habitats such as large, wind-blown dunes (*P. mystaceus* and *P. ornatus–P. interscapularis*
740 groups). Two species of Clade I (*P. scutellatus* and *P. maculatus*) demark independent shifts to
741 firmer ground (clay soils with gravel or salines). Clade II demonstrates adaptation to high
742 elevation, stony or gravel deserts; a reversal to sand habitats occurs for *P. forsythii*, which
743 inhabits the sandy Taklimakan Desert at lower elevations. Clade III likely had a sand-dwelling
744 ancestor (Fig. 7). Many species in this group live on fixed sands with patches of gravel or clay,
745 or they can be observed on various substrates. Some species switch to wind-blown dunes (*P.*
746 *axillaris*, *P. melanurus*, *P. przewalskii*) or gravel (*P. alpherakii*, *P. kuschakewitschii*, *P.*
747 *melanurus*, *P. versicolor*, *P. strauchi*). All members of the *P. raddei–P. helioscopus* group are
748 specialized to life on hard substrates (clay, gravel, salines) and show no reversal to sand habitats,
749 with the exception of *P. helioscopus varius*, which occurs in sandy areas of pine forests in the
750 northernmost limit of its distribution in the Altai Region of Russia (Kotlov 2008).

751 **Body size evolution.** *Phrynocephalus* show significant variation in body size ranging
752 from 35–37 mm (*P. ornatus vindumi*) to 123 mm (*P. mystaceus*) (Supplementary Table S6). The
753 weighted squared-change parsimony algorithm serves to reconstruct the evolution of maximum
754 SVL in *Phrynocephalus* and outgroup Agaminae (Fig. 8). Accordingly, rock-dwelling or
755 climbing forms such as *Agama*, *Trapelus* and *Laudakia* s.l. have larger SVLs than strictly
756 ground-dwelling *Bufoniceps*, *Xenagama* and *Phrynocephalus*. Body size decreases early in the
757 history of *Phrynocephalus*, suggesting that initial miniaturization of its common ancestor was
758 advantageous in wind-blown sand habitats. Strict sand-dwellers, *Microphrynocepahlus* (*P.*
759 *ornatus–P. interscapularis* group) found in the aeolian sand dunes of the Middle East and Turan
760 are the most miniaturized group of *Phrynocephalus* ($SVL_{max} < 47$ mm). An example of an overt
761 reversal in body size occurs in *P. mystaceus*, which is the largest member of the genus and is also
762 specialized to large floating sand dunes. Similar change in body size possibly took place in
763 psammophilous *P. euptilopus*, which appears to be closely related to *P. interscapularis–P.*
764 *luteoguttatus*, but is much larger (SVL_{max} 63 mm) (Alcock & Finn 1897; Arnold 1999). Some
765 species adapted to hard substrates also show an increase in body size, such as *P. maculatus*
766 (SVL_{max} 91 mm) and *P. putjatai* (SVL_{max} 84 mm).

Historical biogeography

Time-tree and origin of *Phrynocephalus*. Estimates of divergence and diversification times for *Phrynocephalus* vary among authors. Macey *et al.* (1993) based on allozymes assumed that *Phrynocepalus* represented an ancient radiation and diverged about 35 Ma. According to immunological data, Ananjeva and Sokolova (1990) estimated the divergence of *Phrynocephalus* from other Agaminae took place around 11 Ma, while their allozyme data provided an estimate of 6 Ma. Using relaxed clock dating, Guo and Wang (2007) suggested a mid-Miocene origin (13.87 Ma, 95% CI 8.5–20.5). Estimates by Melville *et al.* (2009) were older and varied for mtDNA and nuDNA datasets. Their mtDNA suggested all *Phrynocephalus* including *P. interscapularis* diverged 28.9 Ma (21.1–36.2 Ma). Excluding *P. interscapularis*, the estimated origin dated to 22.4 Ma (16.5–30.6 Ma) for mtDNA, and 15.8 Ma (11.8–23.0 Ma) for nuDNA.

Our analyses based on mtDNA data suggest that the ancestor of *Phrynocephalus* diverged from other Agaminae in early Oligocene around 33.2 Ma (19.92–45.69 Ma), or based on nuDNA data in late Oligocene around 26.9 Ma (22.44–31.27 Ma). The basal differentiation within the genus took place in early Miocene (mean 19.3 Ma; 95% CI 12.20–28.90 Ma) or mid-Miocene (mean 14.76 Ma; 95% CI 12.01–17.47 Ma) based on mtDNA and nuDNA data, respectively (Supplementary Table S10). Due to absence of a reliable fossil record of *Phrynocephalus*, all of our calibration nodes correspond to relatively old splits between outgroup taxa, which can potentially result in biased date estimates (see, e.g. Brochu 2004; Hugall *et al.* 2007).

Our estimates best fit the results of Melville *et al.* (2009), but are slightly younger. Melville *et al.* (2009) used one biogeographic and four fossil calibrations, including the enigmatic *Bharatagama* from Early–Middle Jurassic of peninsular India, which is interpreted as a putative stem acrodont (Evans *et al.* 2002). However, the attribution of this fossil is questionable (Townsend *et al.* 2011) and our calibration scheme does not include it (Supplementary Table S5).

Biogeographic history of *Phrynocephalus* and Cenozoic climate change. *Phrynocephalus* is a characteristic element of the deserts of Palearctic Asia, and there is a substantial sympatry between species and species groups (Arnold 1999) (Supplementary Fig. S4). Several hypotheses have been invoked to explain the current broad distribution of the genus. Nikolsky (1916) assumed a Central Asian or Tibetan origin based on remarkable morphological diversity of Central Asian species ("northern origin" hypothesis). Ananjeva and Tuniyev (1992)

798   speculated that there were two original centers for the species of *Phrynocephalus* in the former
799   USSR: Central Asia in the north and Middle Asia in the south. However, their complex
800   hypothesis is not based on an estimated phylogeny and it omits numerous species of
801   *Phrynocephalus* unique to Southwest Asia and China (Kamali & Anderson 2015). Macey *et al.*
802   (1993) suggested that the origins of *Phrynocephalus* trace back to Indian collision with Eurasia
803   35 Ma. Later Arnold (1999) suggested that *Phrynocephalus* evolved in the southern margins of
804   the present distribution, i.e. in the Arabia–NW India area rather than in Central Asia ("southern
805   origin" hypothesis). Some researchers (Wang & Macey 1993; Zeng *et al.* 1997; Pang *et al.* 2003)
806   argued that the basal differentiation of *Phrynocephalus* and the origin of the viviparous species
807   group resulted from vicariance associated with the uplifting of the QTP. Guo and Wang (2007)
808   suggested that *Phrynocephalus* diversified in the Late Miocene to Pleistocene from centers of
809   origin in temperate deserts of Central Asia, and the Tarim and Junggar basins. Several rapid
810   speciation events followed this in a relatively short time (northern origin hypothesis). However,
811   despite recent progress based on molecular phylogenetics (Pang *et al.* 2003; Melville *et al.* 2009;
812   Guo & Wang 2007), our understanding of the biogeography of *Phrynocephalus*, especially of the
813   oviparous taxa inhabiting Middle Asia and South-Western Asia, remains very poor.

814   *Phrynocephalus* belongs to the subfamily Agaminae, which is hypothesized to have
815   originated in Afro-Arabia and colonized Eurasia during a slow closure of the Tethys following
816   movement of Arabian plate northwards (Macey *et al.* 2000). The landbridge connecting Afro-
817   Arabia with Eurasia (known as "*Gomphotherium*-landbridge" or GLB; Figs. 5 and 6) was formed
818   around 18–17 Ma and it facilitated a great faunal exchange between these landmasses (Rögl
819   1998; Rögl 1999). After a temporary disruption, the landbridge has persisted continuously since
820   the mid-Miocene about 15 Ma (Harzhauser 2007; Pook *et al.* 2009; Metallinou *et al.* 2012;
821   Scherler *et al.* 2013; Šmíd *et al.* 2013). Our analyses strongly suggest that the ancestor of
822   *Phrynocephalus* diverged from other agamines around 27 Ma in late Oligocene, or ca. 9–10
823   million years predating the first connection of Afro-Arabia with Eurasia. Because Asian
824   agamines are not monophyletic with respect to African taxa, if Macey *et al.*'s (2000; 2006)
825   hypothesis on an Afro-Arabian origin of the subfamily is correct, then the ancestor of
826   *Phrynocephalus*, *Laudakia* and *Trapelus* + *Bufoniceps* should have colonized Asia
827   independently from Arabia before formation of the GLB. Because Agamidae and putative
828   Agaminae were present in Asia starting from the Late Cretaceous and early Cenozoic (Estes

829 1983; Borsuk-Białynicka & Moody 1984; Alifanov 1989; Borsuk-Białynicka 1996; Prasad &

830 Bajpaj 2008), we cannot exclude an Asian origin of Agaminae with subsequent colonization of

831 Africa. The oldest known fossil of *Phrynocephalus* is reported from eastern Turkey (Zerova &

832 Chkhikvadze 1984); this record is quite young quite young (ca. 5 Ma) and not reliable. The

833 driver of the basal differentiation within Agaminae in Oligocene (ca. 29 Ma) remains an enigma,

834 as does the distribution of the common ancestor of *Phrynocephalus* (Fig. 5).

835 Figure 5 shows the main events in biogeographic history of *Phrynocephalus* inferred

836 from molecular analyses and paleorange reconstructions. The basal radiation of *Phrynocephalus*

837 happened around 14.8 Ma and likely took place in Middle East or southern Middle Asia (Turan)

838 (Fig. 5). This scenario cannot reject the "southern origin" hypothesis for *Phrynocephalus*, as it

839 does for the other hypotheses.

840 One of the most remarkable episodes of global climate evolution during the Cenozoic is

841 the Middle Miocene Climatic Transition (MMCT), which occurred between 14.8 and 14.1 Ma.

842 (Flower & Kennett 1994). At that time, a major and permanent cooling trend replaced the warm

843 and humid tropical or subtropical climate of the Mid-Miocene Thermal Optimum (17–15 Ma;

844 Zachos *et al.* 2001; Böhme 2003). The MMCT saw an increased meridional temperature gradient

845 that strengthened the boundaries between climatic zones and increased aridification of the mid-

846 latitudes (Flower & Kennett 1994). The MMCT was synchronous with the Paratethys salinity

847 crisis (Rögl 1999), which was a major drying of the Paratethys Sea that may have formed

848 significant wind-blown sand and evaporitic desert areas in Middle Asia. The MMCT

849 aridification trend facilitated the spread of drier landscapes over the Mediterranean Basin, Arabia,

850 the Iranian Plateau and Middle Asia and promoted dispersal of xerophilic species (Manafzadeh

851 *et al.* 2014). The basal radiation of *Phrynocephalus* into clades I–III coincides perfectly with

852 onset of the MMCT (14.8 Ma). The increasing aridification provided a diversity of desert

853 habitats for *Phrynocephalus* to occupy as they started to disperse out of the ancestral area in

854 Middle East and Turan (Fig. 5). A similar pattern was recently shown for agamid fan-throated

855 lizards (genus *Sitana* Cuvier, 1829), which diversified in response to ongoing aridification of the

856 Indian subcontinent in the late Miocene (Deepak & Karanth 2018).

857 The ancestors of viviparous *Oreosaura* (Clade II) supposedly colonized the QTP 13.5–

858 10.0 Ma and diversification within this clade began around 3.8 Ma ago (Figs. 5 and 6). Our

859 estimated divergence for *Oreosaura* is older than the earlier estimate of 9.7 Ma (95% interval:

860 7.2–13.0 Ma) by Jin and Brown (2013). Our date coincides with hypothesized major uplifting of
861 the QTP (Shackleton & Chang 1988) and, thus, is consistent with the view that viviparity
862 evolved when this clade became restricted to regions of high elevation. The orogenesis of Tibet
863 is traditionally regarded as the main driving force of Asian monsoons system and subsequent
864 cooling and progressive aridization in Central Asia (Ramstein *et al.* 1997). However, recent
865 works raise a doubt on the Miocene uplifting of the QTP, suggesting that Tibet has been 4–5 km
866 high since the mid-Eocene (ca. 40 Ma), while Indian and Southeast Asian summer monsoons,
867 and Central Asian winter monsoons arose at different times and are unrelated to Tibetan
868 orogenesis (reviewed by Renner 2016). These new data necessitate significant reconsideration of
869 QTP historical biogeography and *Phrynocephalus* may represent a promising model group for
870 such studies.

871 Oviparous clades I and III remained largely within the hypothetical ancestral range of
872 *Phrynocephalus* (Middle East and Turan) (Fig. 5 and 6). Clade I has its highest diversity in the
873 Iranian Plateau and adjacent parts of the Middle East. The ancestor of *P. mystaceus* diverged
874 around 11.3 Ma; this large-sized psammophilous species spread northwards to Turan, Middle
875 Asia and the Caspian Basin where vast areas of wind-blown sand deserts were formed after
876 gradual drying up of the Paratethys Sea. Simultaneously, an ancestor of the *P. arabicus–P.*
877 *maculatus* group occupied deserts of the Arabian Peninsula between 10 and 5 Ma (Fig. 5). The
878 vicariant divergence between the ancestor of *P. arabicus* + *P. longicaudatus* from the Near East
879 and Iranian *P. maculatus* happened around 4.8 Ma. This coincides with intensive uplifting of the
880 Zagros Mountains in western Iran around 7 to 5 Ma ago (Moutherau *et al.* 2012).

881 Oviparous clade III encompasses the highest number of species and has the largest
882 distribution in ranging from the Middle East and Asia Minor to Turan and Middle and Central
883 Asia. Cladogenesis started in the Late Miocene (ca. 8.9–7.1 Ma) and was likely influenced by
884 progressive aridification of central Eurasia, orogenesis and changes in level of the Paratethys Sea.
885 The age of the Central Asian deserts is questionable. The 22 Ma estimation of the onset of
886 aridification in northwestern China (Xia & Hu 1993; Guo *et al.* 2002) corresponds with estimates
887 for the basal radiation in Dipodidae (Shenbrot *et al.* 2017), which is the major autochthonous
888 component of Central Asian desert mammal community. The primary center of radiation for
889 *Phrynocephalus* in Southwest Asia best explains their apparent lag in radiation.

890   The *P. raddei–P. helioscopus* group adapted to life on gravel or clay deserts. The highest
891   diversity within this group occurs on alluvial plains of Middle Asia and Turan. The *P.*
892   *helioscopus–P. persicus* species complex has largest distribution penetrating westwards to
893   Transcaucasia and eastern Asia Minor, and northwards to the Caspian Basin, lowland deserts of
894   Middle and Central Asia as far as western Mongolia (Fig. 5). Orogenetic processes in the Iranian
895   Plateau and Kopet Dagh Mountains (Smit *et al.* 2013) possibly shaped the initial splits (6.2–3.4
896   Ma). The common ancestor of the *P. axillaris* and *P. guttatus–P. versicolor* group likely
897   dispersed to Central Asia around 8.5 to 7 Ma, where it diversified. Accordingly, *P. axillaris*
898   appears to have remained in the Taklimakan Basin and adjacent parts of Tibet, where
899   desertification started from at least 22.6 Ma ago (Zheng *et al.* 2015). The ancestors of the *P.*
900   *guttatus–P. versicolor* group penetrated to Middle Asia (Dunayev 2009). Divergence between *P.*
901   *guttatus* and *P. versicolor* species complexes occurred around 3.8 Ma, and this may coincide
902   with accelerated uplifting of the Altai and Tianshan mountains around 5.0 to 3.1 Ma (Avouac *et*
903   *al.* 1993; Abdrakhmatov *et al.* 1996; Charreau *et al.* 2005; Yuan *et al.* 2006). The ancestors of *P.*
904   *guttatus* and *P. moltschanovi* further spread westwards, occupying the Caspian Basin and north-
905   western Turan (Fig. 5).

906   Plio-Pleistocene glacial cycling likely profoundly affected subsequent radiations and
907   range expansions within species complexes occupying northern parts of Middle and Central Asia
908   (Aubekerov & Gorbunov 1999). Formation of local montane glaciers or permafrost areas during
909   glacial maximums could have led to the retreat of *Phrynocephalus* to warmer refugia followed
910   by subsequent dispersals in warmer periods (Melville *et al.* 2009). Apparently, the QTP, now
911   home to an impressive radiation of viviparous *Oreosaura*, was covered by a thick ice sheet in the
912   Pleistocene (Kuhle 1998). Hence, their distributions and the role they played in shaping the
913   Central Asian biota remains insufficiently understood and requires further studies.

914

Conclusions

916   Exhaustive taxonomic sampling of *Phrynocephalus* is challenging. Some species of
917   *Phrynocephalus* are only known from the type specimens and old collections (e.g. *P. euptilopus*
918   and *P. nasatus*) (Barabanov & Ananjeva 2005), while others occur in politically unstable zones
919   (e.g. deserts of Pakistan, Afghanistan, and Taklamakan). Our analyses provide the most
920   comprehensive taxonomic and gene sampling for *Phrynocephalus* to date. We evaluate 32

nominal taxa using four mtDNA and four nuDNA protein-coding genes. The sampling comprises over four-fifths of the species and covers the distribution of the genus. The mtDNA and nuDNA trees clarify the initial cladogenesis of these lizards. Statistically significant mito-nuclear discordance occurs likely due to hybridization and the introgression of mitogenomes. Analyses shed light on a number of taxonomic issues. Our results contribute to the interpretation of diversification patterns of Central Asian arid zone lizards and provides insights into the historical biogeography of this region.

Analyses confirm the monophyly of *Phrynocephalus* and infer its biogeographic history. The ancestral area of the Agaminae and factors that influenced its diversification remains uncertain. The origin of *Phrynocephalus* dates to the Late Oligocene (26.9 Ma) and this precedes the formation of the Mid-Miocene landbridge that connected Africa and Asia. The common ancestor of *Phrynocephalus* appears to have been a ground-dwelling, miniaturized agamine adapted to sand habitats. The basal divergence of *Phrynocephalus* into three major clades appears to have occurred in the Middle East or southern Middle Asia (Turan) around 14.8 Ma. This corresponds well with the Mid-Miocene Climatic Transition—climate cooling that coincided with aridification and spreading of xerophytic plants across Mediterranean and Paratethys Basins. Subsequent drying up of the Paratethys Sea formed vast desert habitats that *Phrynocephalus* appears to have occupied. Two oviparous clades dispersed independently to lowland deserts of the Arabian Peninsula, Middle and Central Asia. Orogenetic processes and Paratethys Basin dynamics appear to have driven further cladogenesis, which Pliocene–Pleistocene climate oscillations built upon. Substantial variation in body size and morphology occurs in the oviparous lizards. Viviparous *Oreosaura* occupied the QTP around 13.5–10 Ma. Cladogenesis in this group dates between the late Oligocene and mid-Pliocene depending on the dataset (3.8 Ma from nuDNA, 6.4 Ma from mtDNA). This estimate coincides well with the divergence time of another viviparous group of lizards inhabiting Central Asia—the racerunner subgenus *Pareremias* (Lacertidae) (Orlova *et al.* 2017), which was dated to about 6.3 Ma from mtDNA data (Guo *et al.* 2011).

Climatic changes during the Cenozoic, including the ongoing aridification of central Eurasia, shaped the biodiversity of the region (e.g., Peng *et al.* 2006; Yang *et al.* 2006; Jin *et al.* 2008; Melville *et al.* 2009; Guo *et al.* 2011; Jin & Brown 2013; Pisano *et al.* 2015). Most recent biogeographic studies assume the hypothesis that speciation in Central Asia correlated with the

952 evolution of an East Asian monsoon climate triggered by the rapid uplifting of the QTP
953 (Harrison *et al.* 1992; Harrison *et al.* 1995; An *et al.* 2001; Molnar 2005). However,
954 biogeographic histories of many taxa, including those inhabiting Central Asia and the QTP,
955 might require reconsideration due to conflicting hypotheses on geological and climatic history of
956 the region (Renner 2016). Accordingly, our study highlights the importance of Cenozoic
957 paleogeographic and paleoclimatic events in the diversification of Palaearctic lizards.

958

Acknowledgements

960 The authors are grateful to the following colleagues who took part in the fieldwork, collected
961 material and discussed the results, assembled and facilitated obtaining samples, as well as
962 providing access to collections: V.F. Orlova, E.V. Vashetko, M.A. Chirikova, Weiwei Zhou, Wei
963 Gao, T.N. Duysebayeva, P.V. Kvartalnov, T.A. Nazhmudinov, M.N. Yakubov, L.A. Neymark,
964 A.A. Vedenin, I.V. Artyushin, and E.A. Peregontsev. NAP thanks Alexandra A. Elbakyan for
965 help with accessing required literature.

966

References

Abdrakhmatov KY, Aldazhanov SA, Hager BH, Hamburger MW, Herring TA, Kalabaev KB, Makarov VI, Molnar P, Panasyuk SV, Prilepin MT, Reilinger RE, Sadybakasov IS, Souter BJ, Trapeznikov YA, Tsurkov VY, Zubovich AV. 1996. Relatively recent construction of the Tien Shan inferred from GPS measurements of present day crustal deformation rates. *Nature* 384:450–453. https://doi.org/10.1038/384450a0

Alcock AW, Finn F. 1897. An account of the Reptilia collected by Dr. F.P. Maynard, Captain A.H. McMahon, C.I.E., and the members of the Afghan–Baluch Boundary Commission of 1896. *Journal of the Asiatic Society of Bengal* 65:550–566. [1896]

Alifanov VR. 1989. New Priscagamida [sic] (Lacertilia) from the Upper Cretaceous of Mongolia and their systematic position among Iguania. *Paleontological Journal* 1989: 68–80. [in Russian]

An Z, Kutzbach JE, Prell WL, Porter SC. 2001. Evolution of Asian monsoons and phased uplift of the Himalaya–Tibetan Plateau since late Miocene times. *Nature* 411:62–66. https://doi.org/10.1038/35075035

Ananjeva NB, Orlov NL, Khalikov RG, Darevsky IS, Ryabov SA, Barabanov AV. 2006. *The Reptiles of Northern Eurasia*. Pensoft Series Faunistica 245.

Ananjeva NB, Sokolova TM. 1990. The position of the genus *Phrynocephalus* Kaup 1825 in agamids system. *Trudy Zoologicheskogo Instituta Akademii Nauk SSSR* 207:12–21. [in Russian]

Ananjeva NB, Tuniev BS. 1992. Historical biogeography of the *Phrynocephalus* species of the USSR. *Asiatic Herpetological Research* 4:76–98.

Ananjeva NB. 1987. On the validity of *Megalochilus mystaceus* (Pallas, 1776). In: Ananjeva NB, Borkin LJ, Eds. Systematics and Ecology of Amphibians and Reptiles. *Proceedings of the Zoological Institute USSR Academy of Sciences Leningrad* 157:4–13. [in Russian]

Arévalo E, Davis SK, Sites JW Jr. 1994. Mitochondrial DNA sequence divergence and phylogenetic relationships among eight chromosome races of the *Sceloporus grammicus* complex (Phrynosomatidae) in central Mexico. *Systematic Biology* 43:387–418. https://doi.org/10.1093/sysbio/43.3.387

Arnold EN. 1999. Phylogenetic relationships of toad-headed lizards (*Phrynocephalus*, Agamidae) based on morphology. *Bulletin of the British Museum (Natural History), Zoology* 65(1,3):1–13.

Arnold EN. 1992. The Radjasthan toad-headed lizard, *Phrynocephalus longwalensis* (Reptilia: Agamidae) represents a new genus. *Journal of Herpetology* 26:467–472.

Aubekerov B, Gorbunov A. 1999. Quaternary permafrost and mountain glaciation in Kazakhstan. *Permafrost and Periglacial Processes* 10:65–80.

Avouac J-P, Tapponnier P, Bai P, You M, Wang G. 1993. Active thrusting and folding along the northern Tien Shan and late Cenozoic rotation of the Tarim relative to Dzungaria and Kazakhstan. *Journal of Geophysical Research* 98:11791– 11808.

Bannikov AG, Darevsky IS, Ischchenko VG, Rustamov AK, Szczerbak NN. 1977. *Opredelitel Zemnovodnikh i Presmikayushchikhsya Fauni SSSR* [Guide to the Reptile and Amphibian Fauna of the USSR]. Enlightenment Publ., Moscow, USSR 414. [in Russian]

Barabanov AV, Ananjeva NB. 2007. Catalogue of the available scientific species-group names for lizards of the genus *Phrynocephalus* Kaup, 1825 (Reptilia, Sauria, Agamidae). *Zootaxa* 1399: 1–56. https://doi.org/10.11646/zootaxa.1399.1.1

Böhme M. 2003. The Miocene climatic optimum: evidence from ectothermic vertebrates of Central Europe. *Palaeogeography, Palaeoclimatology, Palaeoecology* 195:389–401. https://doi.org/10.1016/S0031-0182(03)00367-5

Borsuk-Białynicka M, & Moody SM. 1984. Priscagaminae, a new subfamily of the Agamidae (Sauria) from the Late Cretaceous of the Gobi Desert. *Acta Palaeontica Polonica* 29:51–81.

Borsuk-Białynicka M. 1996. The Late Cretaceous lizard *Pleurodontagama* and the origin of tooth permanency in Lepidosauria. *Acta Palaeontologica Polonica* 41(3):231–252.

Brochu CA. 2004. Calibration age and quartet divergence date estimation. *Evolution* 58(6):1375–1382.

Burland TG. 1999. DNASTAR's Lasergene Sequence Analysis Software. *Methods in Molecular Biology* 132:71–91. https://doi.org/10.1385/1-59259-192-2:71

1024 Cerling TE, Harris JM, MacFadden BJ, Leakey MG, Quade J, Eisenmann V, Ehleringer JR.
1025   1997. Global vegetation change through the Miocene/Pliocene boundary. *Nature*
1026   389:153–158. https://doi.org/10.1038/38229

1027 Charreau J, Chen Y, Gilder S, Dominguez S, Avouac J-P, Sen S, Sun D, Li Y, Wang W-M. 2005.
1028   Magnetostratigraphy and rock magnetism of the Neogene Kuitun He section (northwest
1029   China): implications for Late Cenozoic uplift of the Tianshan Mountains. *Earth and*
1030   *Planetary Science Letters* 230:177– 192. https://doi.org/10.1016/j.epsl.2004.11.002

1031 Chernov SA. 1948. Reptiles — Reptilia. In: Pavlovsky EN, Vinogradova BS, Eds. *The Animals*
1032   *of the USSR*. Vol. 2. The desert zone. Published by USSR Academy of Sciences,
1033   Moscow-Leningrad 127–161. [in Russian].

1034 Chernov SA. 1959. *Reptilia. Fauna of Tajik USSR*. Dushanbe 48:203. [in Russian]

1035 Clemann N, Melville J, Ananjeva NB., Scroggie MP, Milto K, Kreuzberg E. 2008. Microhabitat
1036   occupation and functional morphology of four species of sympatric agamid lizards in the
1037   Kyzylkum Desert, central Uzbekistan. *Animal Biodiversity and Conservation* 31(2):1–12.

1038 Deepak V, Karanth P. 2018. Aridification driven diversification of fan-throated lizards from the
1039   Indian subcontinent. *Molecular Phylogenetics and Evolution* 120(2018): 53–62.
1040   https://doi.org/10.1016/j.ympev.2017.11.016

1041 Drummond AJ, Suchard MA, Xie D, Rambaut A. 2012. Bayesian phylogenetics with BEAUti
1042   and the BEAST 1.7. *Molecular Biology and Evolution* 29(8):1969–1973.
1043   https://doi.org/10.1093/molbev/mss075.

1044 Dunayev EA. 1995. Reviewed description of the types of *Phrynocephalus strauchi* Nikolsky,
1045   1899 (Squamata, Agamidae) and materials on the history of its study, distribution, and
1046   variability. *Russian Journal of Herpetology* 2(2):87–94.

1047 Dunayev EA. 1996. On the possible use of the ethological features in the taxonomy and
1048   phylogeny of toad agamas. *Russian Journal of Herpetology* 3(1):32–38.

1049 Dunayev EA. 1996. Nomenclature and distribution of toad-agamas, *Phrynocephalus* (Reptilia,
1050   Agamidae) in Iliyskaya Hollow. *Bulletin of the Moscow Society of Naturalists, Biology*
1051   *Ser., Moscow* 101(3):36–41. [in Russian]

1052 Dunayev EA. 2007. Phylogeny of lizards of *Phrynocephalus* genus (Reptilia: Agamidae): history
1053   of study and methodic approaches. *Voprosy Gerpetologii* 105–114. [in Russian]

1054 Dunayev EA. 2009. Systematics and paleogeography: conceptual synthesis by the example of
1055   *Phrynocephalus* (superspecies *guttatus*) (Reptilia: Agamidae). In: Sviridov AV, Shatalkin
1056   AI, Eds. Evolution and Systematics: Lamarck and Darwin in modern studies. Archiver of
1057   the Zoological Museum of Moscow State University. Vol. L. Moscow: KMK scientific
1058   press 274–298. [in Russian]

1059 Eichwald DE. 1831 *Zoologia specialis quam expozitis animalibus tum vivis, tum fossilibus*
1060   *potissimus rossiae in universum, et poloniae in specie*. Posterior, specialem expositionem
1061   Spondylozoorum continens. Vilnius 404.

1062 Eremchenko V, Panfilov A. 1999. Some question of methodology of taxonomy and phylogeny of
1063   toad agamas on the example of *Phrynocephalus helioscopus* (Pallas, 1771) (Sauria:
1064   Agamidae). *Nauka i Noviye Tekhnologii*, Bishkek 3:116–122 [in Russian with English
1065   summary].

1066 Estes R. 1983. Sauria Terrestria, Amphisbaenia (Handbuch der Paläoherpetologie, v. 10A).
1067   Stuttgart. Gustav Fischer Verlag: 249.

1068 Evans SE, Prasad GVR, Manhas BK. 2002. Fossil lizards from the Jurassic Kota formation of
1069   India. *Journal of Vertebrate Paleontology* 22:299–312. https://doi.org/10.1671/0272-
1070   4634(2002)022[0299:FLFTJK]2.0.CO;2

1071 Farris JD, Kallersjo M, Kluge AG, Bult C. 1994. Testing significance of incongruence.
1072   *Cladistics* 10:315–319. https://doi.org/10.1111/j.1096-0031.1994.tb00181.x

1073 Farris JD, Kallersjo M, Kluge AG, Bult C. 1995. Constructing a significance test for
1074   incongruence. *Systematic Biology* 44:570–572. https://doi.org/10.1093/sysbio/44.4.570

1075 Felsenstein J. 2004. *Inferring phylogenies*. Vol. 2. Sinauer Associates, Inc. Publishers,
1076   Sunderland, Massachusetts, 465 pp.

1077 Fisher-Reid MC, Wiens JJ. 2011. What are the consequences of combining nuclear and
1078   mitochondrial data for phylogenetic analysis? Lessons from *Plethodon* salamanders and
1079   13 other vertebrate clades. *BMC Evolutionary Biology* 11:300.
1080   https://doi.org/10.1186/1471-2148-11-300

1081 Flower BP, Kennett JP. 1994. The Middle Miocene climatic transition: East Antarctic ice sheet
1082   development, deep ocean circulation and global carbon cycling. *Palaeogeography,*

1083   *Palaeoclimatology, Palaeoecology* 108:537–555. https://doi.org/10.1016/0031-
1084   0182(94)90251-8

1085 Golonka J. 2004. Plate tectonic evolution of the southern margin of Eurasia in the Mesozoic and
1086   Cenozoic. *Tectonophysics* 381(1):235–273. https://doi.org/10.1016/j.tecto.2002.06.004

1087 Golubev ML, Gorelov YK, Dunayev EA, Kotenko TI. 1995. On the finding of *Phrynocephalus*
1088   *guttatus* (Gmel.) (Sauria, Agamidae) in Turkmeniya and its taxonomic status. *Bulletin of*
1089   *the Moscow Society of Naturalists [Bulleten Moskovskogo Obschestva Ispytateley*
1090   *Prirody], Otdel Biologicheskiy* 100(3):31–39 [in Russian with English summary].

1091 Golubev ML. 1991. About the name *Agama ocellata* Lichtenstein In Eversmann, 1823 (Reptilia,
1092   Agamidae) with redescription of the types. *Herpetological Researches.* Leningrad 1:12–
1093   17. [in Russian]

1094 Golubev ML. 1993. The variegated toad agama in Djungar Gate (Eastern Kazakstan) with notes
1095   on certain systematic problems of *Phrynocephalus versicolor* str. (Reptilia: Agamidae).
1096   *Asiatic Herpetological Research* 5:51–58.

1097 Gozdzik A, Fu J. 2009. Are toad-headed lizards *Phrynocephalus przewalskii* and *P. frontalis*
1098   (family Agamidae) the same species? Defining species boundaries with morphological
1099   and molecular data. *Russian Journal of Herpetology* 16 (2):107–118.

1100 Guo X, Dai X, Chen D, Papenfuss T, Ananjeva NB, Melnikov DA, Wang Y. 2011. Phylogeny
1101   and divergence times of some racerunner lizards (Lacertidae: *Eremias*) inferred from
1102   mitochondrial 16S rRNA gene segments. *Molecular Phylogenetics and Evolution*
1103   61(2):400–412. https://doi.org/10.1016/j.ympev.2011.06.022

1104 Guo X, Wang Y. 2007. Partitioned Bayesian analyses, dispersal-vicariance analysis, and the
1105   biogeography of Chinese toad-headed lizards (Agamidae: *Phrynocephalus*): a re-
1106   evaluation. *Molecular   Phylogenetics   and   Evolution*   45(2):643–662.
1107   https://doi.org/10.1016/j.ympev.2007.06.013

1108 Guo ZT, Ruddiman WF, Hao QZ, Wu HB, Qiao YS, Zhu RX, Peng SZ, Wei JJ, Yuan BY, Liu
1109   TS. 2002. Onset of Asian desertification by 22 Myr ago inferred from loess deposits in
1110   China. *Nature* 416:159–163. https://doi.org/10.1038/416159a

1111 Haas G. 1957. Some amphibians and reptiles from Arabia. *Proceedings of the California*
1112   *Academy of Sciences* 29(3):47–86.

1113 Hall TA. 1999. BioEdit: a user-friendly biological sequence alignment editor and analysis
1114   program for Windows 95/98/NT. *Nucleotide* 41:95–98.

1115 Harrison TM, Copeland P, Kidd WSF, Loevera OM. 1995. Activation of the Nyainqentanghla
1116   shear zone: implications for uplift of the southern Tibetan Plateau. *Tectonics* 14:658–676.
1117   https://doi.org/10.1029/95TC00608

1118 Harrison TM, Copeland P, Kidd WSF, Yin A. 1992. Raising Tibet. *Science* 255:1663–1670.

1119 Harzhauser M, Kroh A, Mandic O, Piller WE, Göhlich U, Reuter M, Berning B. 2007.
1120   Biogeographic responses to geodynamics: a key study all around the Oligo-Miocene
1121   Tethyan Seaway. *Zoologischer Anzeiger-A Journal of Comparative Zoology* 246:241–
1122   256. https://doi.org/10.1016/j.jcz.2007.05.001

1123 Heled J, Drummond AJ. 2010. Bayesian inference of species trees from multilocus data.
1124   *Molecular Biology and Evolution* 27:570. https://doi.org/10.1093/molbev/msp274

1125 Huelsenbeck JP, Hillis DM. 1993. Success of phylogenetic methods in the four-taxon case.
1126   *Systematical Biology* 42:247–264. https://doi.org/10.1093/sysbio/42.3.247

1127 Hugall AF, Foster R, Lee MS. 2007. Calibration choice, rate smoothing, and the pattern of
1128   tetrapod diversification according to the long nuclear gene RAG-1. *Systematic Biology*
1129   56(4):543–563.

1130 ICZN. 1999. *International Code of Zoological Nomenclature*. Fourth edition. The International
1131   Trust for Zoological Nomenclature, London, UK. BHL. The Code Online (ICZN).

1132 Ivanova NV, DeWaard J, Hebert PDN. 2006. An inexpensive, automation friendly protocol for
1133   recovering high quality DNA. *Molecular Ecology Notes* 6:998–1002.
1134   https://doi.org/10.1111/j.1471-8286.2006.01428.x

1135 Jin Y-T, Brown RP, Liu N-F. 2008. Cladogenesis and phylogeography of the lizard
1136   *Phrynocephalus vlangalii* (Agamidae) on the Tibetan Plateau. *Molecular Ecology*
1137   17:1971–1982. https://doi.org/10.1111/j.1365-294X.2008.03721.x

1138 Jin Y-T, Brown RP. 2013. Species history and divergence times of viviparous and oviparous
1139   Chinese toad-headed sand lizards (*Phrynocephalus*) on the Qinghai-Tibetan Plateau.
1140   *Molecular Phylogenetics and Evolution* 68:259–268.
1141   https://doi.org/10.1016/j.ympev.2013.03.022

Jin Y-T, Liu N-F. 2010. Phylogeography of *Phrynocephalus erythrurus* from the Qiangtang Plateau of the Tibetan Plateau. *Molecular Phylogenetics and Evolution* 54:933–940. https://doi.org/10.1016/j.ympev.2009.11.003

Jin Y, Liu N, Brown RP. 2017. The geography and timing of genetic divergence in the lizard *Phrynocephalus theobaldi* on the Qinghai-Tibetan Plateau. *Scientific Reports* 7(2281): https://doi.org/10.1038/s41598-017-02674-4.

Jobb G. 2011. *TREEFINDER version of March 2011*. Munich, Germany. Distributed by the author at www.treefinder.de.

Kamali K, Anderson SC. 2015. A new Iranian *Phrynocephalus* (Reptilia: Squamata: Agamidae) from the hottest place on earth and a key to the genus *Phrynocephalus* in southwestern Asia and Arabia. *Zootaxa* 3904 (2):249–260. https://doi.org/10.11646/zootaxa.3904.2.4.

Kotlov AA. 2008. Species composition and distribution of amphibians and reptiles of south-western Kulunda. *Altaiskiy Zoologicheskiy Zhurnal* 2:131–133. [in Russian]

Kuhle M. 1998. Reconstruction of the 2.4 million km2 late Pleistocene ice sheet on the Tibetan Plateau and its impact on the global climate. *Quaternary International* 45:71–108.

Lanfear R, Calcott B, Ho SYW, Guindon S. 2012. PartitionFinder: combined selection of partitioning schemes and substitution models for phylogenetic analyses. *Molecular Biology and Evolution* 29(6):1695–1701. https://doi.org/10.1093/molbev/mss020

Leache AD, Cole CJ. 2007. Hybridization between multiple fence lizard lineages in an ecotone: locally discordant variation in mitochondrial DNA, chromosomes, and morphology. *Molecular Ecology* 16:1035–1054. https://doi.org/10.1111/j.1365-294X.2006.03194.x

Li XZ, Dong GR, Chen HZ, Zheng HB, Jin HL, Jin J. 2001. Uplift processes of the Qinghai-Tibetan Plateau interpreted from the comparison of Yecheng section and Siwalik group. *Journal of Desert Research* 21:354–360. [in Chinese with English abstract]

Likhnova O. 1992. Biochemical systematics of toad agamas *Phrynocephalus* (Agamidae, Reptilia). *Asian Herpetological Meeting*, Huangshan: 46–47.

Lomolino MV, Sax DF, Riddle BR, Brown JH. 2006. The island rule and a research agenda for studying ecogeographical patterns. *Journal of Biogeography* 33(9):1503–1510. https://doi.org/10.1111/j.1365-2699.2006.01593.x

1171 Ma C, Arias EF, Eubanks TM, Fey AL, Gontier A-M, Jacobs CS, Sovers OJ, Archinal BA,
1172   Charlo P. 1998. The international celestial reference frame as realized by very long
1173   baseline interferometry. *The Astronomical Journal* 116: 5–6.
1174   https://doi.org/10.1086/300408

1175 Macey JR, Ananjeva NB, Zhao EM, Wang YZ, Papenfuss TJ. 1993. An allozyme-based
1176   phylogenetic hypothesis for *Phrynocephalus* (Agamidae) and its implications for the
1177   historical biogeography of arid Asia. *Proceedings of the First Asian Herpetological*
1178   *Meeting*, China Forestry Press, Beijing: 349.

1179 Macey JR, Schulte II JA, Fong JJ, Das I, Papenfuss TJ. 2006. The complete mitochondrial
1180   genome of an agamid lizard from the Afro-Asian subfamily Agaminae and the
1181   phylogenetic position of *Buloniceps* and *Xenagama*. *Molecular Phylogenetics and*
1182   *Evolution* 39:291–297. https://doi.org/10.1016/j.ympev.2005.08.020

1183 Macey JR, Schulte JA II, Larson A, Ananjeva NB, Wang Y, Rastegar-Pouyani N, Pethiyagoda R,
1184   Papenfuss TJ. 2000. Evaluating Trans-Tethys migration: an example using acrodont
1185   lizard phylogenetics. *Systematic Biology* 49(2):233.

1186 Maddison WP and Maddison DR. 2017. *Mesquite: a modular system for evolutionary analysis.*
1187   *Version 3.31*. Available at: http://mesquiteproject.org

1188 Maddison WP. 1991. Squared-change parsimony reconstructions of ancestral states for
1189   continuous-valued characters on a phylogenetic tree. *Systematic Zoology* 40(3):304–314.
1190   https://doi.org/10.2307/2992324

1191 Manafzadeh S, Salvo G and Conti E. 2014. A tale of migrations from east to west: the Irano-
1192   Turanian floristic region as a source of Mediterranean xerophytes. *Journal of*
1193   *Biogeography* 41:366–379. https://doi.org/10.1111/jbi.12185

1194 Manilo V.V. 2000. Description of karyotypes of some species and subspecies of the genus
1195   *Phrynocephalus* (Sauria, Agamidae) from Central Asia. *Vestnik zoologii* 34(6):113—118.
1196   [in Russian]

1197 Manilo VV. 2001. Cytogenetic review and evolution of karyotypes in the species of the genus
1198   *Phrynocephalus* Kaup, 1825 (Sauria, Agamidae) from the Eastern Palaearctic.
1199   *Hamadryad* 26(2):227–234.

Manilo VV, Golubev ML. 1993. Karyotype information on some toad agamas of the *Phrynocephalus* species group (Sauria, Agamidae) of the former USSR. *Asiatic Herpetological Research* 5:105–108.

Martins EP. 1999. Estimating of ancestral states of continuous characters: a computer simulation study. *Systematic Biology* 48:642–650.

McGuire JA, Linkem CW, Koo MS, Hutchison DW, Lappin AK, Orange DI, Lemos-Espinal J, Riddle BR, Jaeger JR. 2007. Mitochondrial introgression and incomplete lineage sorting through space and time: phylogenetics of crotaphytid lizards. *Evolution* 61: 2879–2897. https://doi.org/10.1111/j.1558-5646.2007.00239.x

Melnikov DA, Melnikova E, Nazarov R, Rajabizadeh M, Al-Johany A, Amr ZS, Ananjeva NB. 2014. Taxonomic revision of *Phrynocephalus arabicus* Anderson, 1984 [sic] complex with description of a new species from Ahvaz, southwestern Iran. *Russian Journal of Herpetology* 21(2):149–159.

Melville J, Hale J, Mantziou G, Ananjeva NB, Milto K, Clemann N. 2009. Historical biogeography, phylogenetic relationships and intraspecific diversity of agamid lizards in the Central Asian deserts of Kazakhstan and Uzbekistan. *Molecular Phylogenetics and Evolution* 53:99–112. https://doi.org/10.1016/j.ympev.2009.05.011

Metallinou M, Arnold NE, Crochet PA, Geniez P, Brito JC, Lymberakis P, El Din SB, Sindaco R, Robinson M, Carranza S. 2012. Conquering the Sahara and Arabian deserts: systematics and biogeography of *Stenodactylus* geckos (Reptilia: Gekkonidae). *BMC Evolutionary Biology* 12:258. https://doi.org/10.1186/1471-2148-12-258

Molnar P. 2005. Mio-Pliocene growth of the Tibetan Plateau and evolution of East Asian climate. *Palaeontologia Electronica* 8(1):1–23.

Moody SM, Hutterer HR. 1978. Karyotypes of the agamid lizard *Lyriocephalus scutatus* (L 1758), with a brief review of the chromosomes of the lizard family Agamidae. *Bönn Zoological Bulletin* 29:165–170.

Moody SM. 1980. *Phylogenetic and historical biogeographical relationships of the genera in the family Agamidae (Reptilia: Lacertilia)*. PhD thesis, Univ. Michigan, Ann Arbor: 373.

Moutherau F, Lacombe O, Vergés J. 2012. Building the Zagros collisional orogen: timing, strain distribution and the dynamics of Arabia/Eurasia Plate convergence. *Tectonophysics* 532–535:27–60. https://doi.org/10.1016/j.tecto.2012.01.022

1231 Ng J, Glor RE. 2011. Genetic differentiation among populations of a Hispaniolan trunk anole
1232   that exhibit geographical variation in dewlap colour. *Molecular Ecology* 20:4302–4317.
1233   https://doi.org/10.1111/j.1365-294X.2011.05267.x

1234 Nguyen SN, Zhou W-W, Le T-NT, Tran A-DT, Jin J-Q, Vo BD, Nguyen LT, Nguyen TT,
1235   Nguyen TQ, Hoang DD, Orlov NL, Che J, Murphy RW, Zhang Y-P. 2017. Cytonuclear
1236   discordance, cryptic diversity, complex histories, and conservation needs in Vietnamese
1237   bent-toed geckos of the *Cyrtodactylus irregularis* species complex. *Russian Journal of*
1238   *Herpetology* 24 (2):133–154.

1239 Nikolsky AM. 1916. *Reptilia. Vol. II. Ophidia. The fauna of Russia and adjacent countries*.
1240   Imperial Academy of Science Press, Petrograd: 349. [in Russian]

1241 Noble DWA, Qi Y, Fu J. 2010. Species delineation using Bayesian model-based assignment tests:
1242   a case study using Chinese toad-headed agamas (genus *Phrynocephalus*). *BMC*
1243   *Evolutionary Biology* 10:197. https://doi.org/10.1186/1471-2148-10-197

1244 Orlova VF, Poyarkov NA, Chirikova MA, Nazarov RA, Munkhbayar M, Munkhbayar Kh,
1245   Terbish Kh. 2017. MtDNA differentiation and taxonomy of Central Asian racerunners of
1246   *Eremias multiocellata-E. przewalskii* species complex (Squamata, Lacertidae). *Zootaxa*
1247   4282(1):001–042. https://doi.org/10.11646/zootaxa.4282.1.1.

1248 Orlova VF, Dunayev EA, Nazarov RA, Terbish Kh, Erdentushig P. 2014. Materials on the south-
1249   western Mongolia herpetofauna. *Sovremennaya Herpetologiya* 14(1/2):32–43. [in
1250   Russian]

1251 Pan Y. 1999. Formation and uplifting of the Qinghai-Tibetan Plateau. *Frontiers of Earth Science*
1252   6:153–163. [in Chinese with English abstract]

1253 Pang J, Wang Y, Zhong Y, Hoelzele AR, Papenfuss TJ, Zeng X, Ananjeva NB, Zhang YP. 2003.
1254   A phylogeny of Chinese species in the genus *Phrynocephalus* (Agamidae) inferred from
1255   mitochondrial DNA sequences. *Molecular Phylogenetics and Evolution* 27:398–409.

1256 Pedall I, Fritz U, Stuckas H, Valdeon A, Wink M. 2010. Gene flow across secondary contact
1257   zones of the *Emys orbicularis* complex in the western Mediterranean and evidence for
1258   extinction and re-introduction of pond turtles on Corsica and Sardinia (Testudines:
1259   Emydidae). *Journal of Zoological Systematics and Evolutionary Research* 49:44–57.
1260   https://doi.org/10.1111/j.1439-0469.2010.00572.x

1261   Peng Z, Ho SYW, Zhang Y, He S. 2006. Uplift of the Tibetan plateau: evidence from divergence
1262   times of glyptosternoid catfishes. *Molecular Phylogenetics and Evolution* 39:568–572.
1263   https://doi.org/10.1016/j.ympev.2005.10.016

1264   Pisano J, Condamine FL, Lebedev V, Bannikova A, Quéré JP, Shenbrot GI, Pages M, Michaux
1265   JR. 2015. Out of Himalaya: the impact of past Asian environmental changes on the
1266   evolutionary and biogeographical history of Dipodoidea (Rodentia). *Journal of*
1267   *Biogeography* 42(5):856–870. https://doi.org/10.1111/jbi.12476

1268   Pook CE, Joger U, Stümpel N, Wüster W. 2009. When continents collide: Phylogeny, historical
1269   biogeography and systematics of the medically important viper genus *Echis* (Squamata:
1270   Serpentes: Viperidae). *Molecular Phylogenetics and Evolution* 53:792–807.
1271   https://doi.org/10.1016/j.ympev.2009.08.002

1272   Popov SV, Akhmeteyev MA, Lopatin AV, Bugrova AM, Sychevskaya EK, Kopp ML, Szherba
1273   IG, Zaporozhets NI, A.S., Andreeva-Grigorovich, Nikolaeva IA. 2009. *Paleogeography*
1274   *and biogeography of Paratethys basin. Vol. I. Late Eocene–Early Miocene*. Nauchny Mir
1275   200. [in Russian]

1276   Popov SV., Rögl F, Rozanov AY, Steininger FF, Shcherba IG, Kovac K. 2004. *Lithological-*
1277   *paleographic maps of Paratethis. 10 maps Late Eocene to Pliocene*. Courier
1278   Forschungsinstitut Senckenberg, Frankfurt 46.

1279   Prasad GVR, Bajpai G. 2008. Agamid lizards from the early Eocene of western India: oldest
1280   Cenozoic lizards from South Asia. *Palaeontology Electronica* 11:1–19.

1281   Qi Y, Yang W, Lu B, Fu J. 2013. Genetic evidence for male-biased dispersal in the Qinghai
1282   toad-headed agamid *Phrynocephalus vlangalii* and its potential link to individual social
1283   interactions. *Ecology and Evolution* 3(5):1219–30. https://doi.org/10.1002/ece3.532

1284   Rahiamian H, Shafiei S, Rastegar Pouyani N, Rastegar Pouyani E. 2015. Phylogenetic
1285   relationships of the gray-toad agama, *Phrynocephalus scutellatus* (Olivier, 1807), species
1286   complex from Iran. *Zootaxa* 3990 (3):369–380.
1287   https://doi.org/10.11646/zootaxa.3990.3.3

1288   Rambaut A, Drummond AJ. 2007. *Tracer v1. 5*. Available at http:// beast.bio.ed.ac.uk/Tracer.

1289   Ramstein G, Fluteau F, Besse F, Joussaume S. 1997. Effect of orogeny, plate motion and land-
1290   sea distribution on Eurasian climate change over the past 30 million years. *Nature*
1291   386:788–795.

1292 Ree RH, Moore BR, Webb CO, Donoghue MJ. 2005. A likelihood framework for inferring the
1293  evolution of geographic range on phylogenetic trees. *Evolution* 59:2299–2311.
1294  https://doi.org/10.1111/j.0014-3820.2005.tb00940.x

1295 Ree RH, Smith SA. 2008. Maximum likelihood inference of geographic range evolution by
1296  dispersal, local extinction, and cladogenesis. *Systematic Biology* 57:4–14.
1297  https://doi.org/10.1080/10635150701883881

1298 Renner S. 2016. Available data point to a 4-km-high Tibetan Plateau by 40 Ma, but 100
1299  molecular-clock papers have linked supposed recent uplift to young node ages. *Journal of*
1300  *Biogeography* 43(8):1479–1487. https://doi.org/10.1111/jbi.12755

1301 Renoult JP, Geniez P, Bacquet P, Benoit L, Crochet P-A. 2009. Morphology and nuclear markers
1302  reveal extensive mitochondrial introgressions in the Iberian Wall Lizard species complex.
1303  *Molecular Ecology* 18:4298–4315. https://doi.org/10.1111/j.1365-294X.2009.04351.x

1304 Rieppel O, Walker A, Odhiambo I. 1992. A preliminary report on a fossil chamaeoleonine
1305  (Reptilia: Chamaeleoninae) skull from the Miocene of Kenya. *Journal of Herpetology*
1306  26:77–80.

1307 Rögl F. 1998. Paleogeographic considerations for Mediterranean and Paratethys seaways
1308  (Oligocene and Miocene). *Annalen des Naturhistorischen Museums in Wien* 99A: 279–
1309  331.

1310 Rögl F. 1999. Mediterranean and Paratethys. Facts and hypotheses of an Oligocene to Miocene
1311  paleogeography (short overview). *Geologica Carpathica* 50(4):339–349.

1312 Ronquist F, Huelsenbeck JP. 2003. MrBayes 3: Bayesian phylogenetic inference under mixed
1313  models. *Bioinformatics* 19(12):1572-1574. https://doi.org/10.1093/bioinformatics/btg180

1314 Scherler L, Mennecart B, Hiard F, Becker D. 2013. Evolutionary history of hoofed mammals
1315  during the Oligocene-Miocene transition in Western Europe. *Swiss Journal of*
1316  *Geosciences* 106:349–369. https://doi.org/10.1007/s00015-013-0140-x

1317 Schulter D, Price T, Mooers AØ, Ludwig D. 1997. Likelihood of ancestor states in adaptive
1318  radiation. *Evolution* 51:1699–1711.

1319 Shackleton RM, Chang C. 1988. Cenozoic uplift and deformation of the Tibetan Plateau: the
1320  geomorphological evidence. *The Geological Evolution of Tibet. Philosophical*
1321  *Transactions of the Royal Society* 327(1594):365–377.

Sharma RC. 1978. A new species of *Phrynocephalus* Kaup (Reptilia: Agamidae) from the Rajasthan Desert, India, with notes on ecology. *Bulletin of the Zoological Survey of India* 1(3):291–294.

Shenbrot G, Bannikova A, Giraudoux P, Quere JP, Raoul F, Lebedev V. 2017. A new recent genus and species of three-toed jerboas (Rodentia: Dipodinae) from China: a living fossil? *Journal of Zoological Systematics and Evolutionary Research*. 55:356–368. https://doi.org/10.1111/jzs.12182

Shi Y, Li J, Li B, Pan B, Fang X, Yao T, Wang S, Cui Z, Li S. 1998. Uplift and environmental evolution of Qinghai-Xizang (Tibetan) Plateau. *Formation, Evolution and Development of Qinghai-Xizang (Tibetan) Plateau*: 73–138. [in Chinese]

Shimodaira H. 2002. An approximately unbiased test of phylogenetic tree selection. *Systematic Biology* 51(3):492–508.

Shoo L, Rose R, Doughty P, Austin JJ, Melville J. 2008. Diversification patterns of pebble-mimic dragons are consistent with historical disruption of important habitat corridors in arid Australia. *Molecular Phylogenetics and Evolution* 48:528–542. https://doi.org/10.1016/j.ympev.2008.03.022

Šmíd J, Carranza S, Kratochvil L, Gvozdik V, Nasher AK, Moravec J. 2013. Out of Arabia: a complex biogeographic history of multiple vicariance and dispersal events in the gecko genus *Hemidactylus* (Reptilia: Gekkonidae). *PLoS ONE* 8(5):1–14. https://doi.org/10.1371/journal.pone.0064018

Smit JHW, Cloetingh SAPL, Burov E, Tesauro M., Sokoutis D, Kaban M. 2013. Interference of lithospheric folding in western Central Asia by simultaneous Indian and Arabian plate indentation. *Tectonophysics* 602:176–193. https://doi.org/10.1016/j.tecto.2012.10.032

Sokolovsky VV. 1975. Karyotypes and taxonomy of lizards of the family Agamidae. *Biologicheskiye issledovaniya na Dalnem Vostoke*, Vladivostok, 107–111. [in Russian]

Solovyeva EA. 2017. The position of *Phrynocephalus rossikowi* (Reptilia, Agamidae) according to mtDNA from old museum specimen. SEH 19th European Congress of Herpetology. Programme and Abstracts. University of Salzburg, 18–23 September 2017:256.

Solovyeva EN, Dunayev EA, Poyarkov NA. 2012. Interspecific taxonomy of sunwatcher toadhead agama species complex (*Phrynocephalus helioscopus*, Squamata). *Zoologicheskiy Zhurnal* 91(11):1377–1396. [in Russian]

Solovyeva EN, Poyarkov NA, Dunayev EA, Duysebayeva TN, Bannikova AA. 2011. Molecular differentiation and taxonomy of the sunwatcher toad headed agama species complex *Phrynocephalus* superspecies *helioscopus* (Pallas 1771) (Reptilia: Agamidae). *Russian Journal of Genetics* 47(7):952–967.

Solovyeva EN, Poyarkov NA, Dunayev EA, Nazarov RA, Lebedev VS, Bannikova AA. 2014. Phylogenetic relationships and subgeneric taxonomy of toad-headed agamas *Phrynocephalus* (Reptilia, Squamata, Agamidae) based on mitochondrial DNA sequence data. *Doklady Biological Sciences* 455:119–124. https://doi.org/10.1134/S0012496614020148

Sun J, Liu T. 2006. The Age of the Taklimakan Desert. *Science* 312(5780):1621. https://doi.org/10.1126/science.1124616

Swofford DL. 2002. *Phylogenetic analysis using parsimony (*and other methods). Version 4*. Sunderland MA Sinauer Associates.

Szczerbak [Shcherbak] NN. 1994. Zoogeographic analysis of reptiles of Turkmenistan. *Biogeography and Ecology of Turkmenistan* 307–328.

Szczerbak NN. 2003. *Guide to the Reptiles of the Eastern Palearctic*. Golubev ML, Ed. Malabar (Florida): Krieger Publishing, 260 p.

Tamura K, Stecher G, Peterson D, Filipski A, Kumar S. 2013. MEGA6: Molecular Evolutionary Genetics Analysis version 6.0. *Molecular Biology and Evolution* 30: 2725–2729. https://doi.org/10.1093/molbev/mst197

Thompson JD, Higgins DG, Gibson TJ. 1994 CLUSTAL W: improving the sensitivity of progressive multiple sequence alignment through sequence weighting, position-specific gap penalties and weight matrix choice. *Nucleic Acids Research* 22(22):4673–80.

Toews DP, Brelsford A. 2012. The biogeography of mitochondrial and nuclear discordance in animals. *Molecular Ecology* 21:3907–3930. https://doi.org/10.1111/j.1365-294X.2012.05664.x

Townsend TM, Alegre RE, Kelley ST, Wiens JJ, Reeder TW. 2008. Rapid development of multiple nuclear loci for phylogenetic analysis using genomic resources: an example

1381 from squamate reptiles. *Molecular Phylogenetics and Evolution* 47(1):129–142.
1382 https://doi.org/10.1016/j.ympev.2008.01.008

1383 Townsend TM, Mulcahy DG, Noonan BP, Sites JW, Kuczynski CA, Wiens JJ, Reeder TW. 2011.
1384 Phylogeny of iguanian lizards inferred from 29 nuclear loci, and a comparison of
1385 concatenated and species-tree approaches for an ancient, rapid radiation. *Molecular*
1386 *Phylogenetics and Evolution* 61(2011):363–380.
1387 https://doi.org/10.1016/j.ympev.2011.07.008

1388 Uetz P, Hošek J. 2016. *The Reptile Database*. Available at http://www.reptile-database.org,
1389 accessed March 23 2016.

1390 Urquhart J, Wang Y, Fu J. 2009. Historical vicariance and male-mediated gene flow in the toad-
1391 headed lizards *Phrynocephalus przewalskii*. *Molecular Ecology* 18:3714–3729.
1392 https://doi.org/10.1111/j.1365-294X.2009.04310.x

1393 Wang Y, Fu J. 2004. Cladogenesis and vicariance patterns in the toad-headed lizard
1394 *Phrynocephalus versicolor* species complex. *Copeia* 2:199–206.
1395 https://doi.org/10.1643/CG-03-082R1

1396 Wang YZ, Macey JR. 1993. On the ecologico-geographic differentiation of Chinese species of
1397 the genus *Phrynocephalus*. *Proceedings of the First Asian Herpetological Meeting* 147.

1398 Weise V. 1974. The slope development and plain formation in the deserts of the Iranian
1399 highlands. *Wurzburger Geographische Arbeiten* 24:21–26.

1400 Wermuth H. 1967. Liste der rezenten Amphibien und Reptilien. Agamidae. *Das Tierreich*
1401 86:127.

1402 Whiteman RS. 1978. Evolutionary history of the lizard genus *Phrynocephalus* (Lacertilia,
1403 Agamidae). M.A. Thesis, Fullerton, California State University 113.

1404 Xia X, Hu W. 1993. The resources and environment in the Taklimakan Desert. *Science in China*
1405 (Series B) 23(8):889–896. [in Chinese]

1406 Yang Z. 2007. PAML 4: phylogenetic analysis by maximum likelihood. *Molecular Biology and*
1407 *Evolution* 24(8):1586–1591. https://doi.org/10.1093/molbev/msm088

1408 Yang SJ, Yin ZH, Ma XM, Lei FM. 2006. Phylogeography of ground tit (*Pseudopodoces*
1409 *humilis*) based on mtDNA: evidence of past fragmentation on the Tibetan plateau.
1410 *Molecular Phylogenetics and Evolution* 41:257–265.
1411 https://doi.org/10.1016/j.ympev.2006.06.003

1412 Yuan W, Carter A, Dong J, Bao Z, An Y, Guo Z. 2006. Mesozoic–Tertiary exhumation history
1413   of the Altai Mountains, northern Xinjiang, China: new constraints from apatite fission
1414   track data. *Tectonophysics* 412:183–193. https://doi.org/10.1016/j.tecto.2005.09.007

1415 Zachos J, Pagani M, Sloan L, Thomas E, Billups K. 2001. Trends, rhythms, and aberrations in
1416   global climate 65 Ma to present. *Science* 292:686–693.
1417   https://doi.org/10.1126/science.1059412

1418 Zarza E, Reynoso VH, Brent C. 2011. Discordant patterns of geographic variation between
1419   mitochondrial and microsatellite markers in the Mexican black iguana (*Ctenosaura*
1420   *pectinata*) in a contact zone. *Journal of Biogeography* 38:1394–1405.
1421   https://doi.org/10.1111/j.1365-2699.2011.02485.x

1422 Zeng XM, Wang YZ, Liu ZJ, Fang ZL, Wu GF, Papenfuss TJ, Macey JR. 1997. Karyotypes of
1423   nine species in the genus *Phrynocephalus*, with discussion of karyotypic evolution of
1424   Chinese *Phrynocephalus*. *Acta Zoologica Sinica* 43:399–410.

1425 Zerova GA, Chkhikvadze VM. 1984. The review of Cenozoic lizards and snakes in USSR. News.
1426   *Georgian SSR Academy of Sciences. Series: Biology* 10:319–325. [in Russian]

1427 Zhang Q, Xia L, He J, Wu Y, Fu J, Yang Q. 2010. Comparison of phylogeographic structure and
1428   population history of two *Phrynocephalus* species in the Tarim Basin and adjacent areas.
1429   *Molecular Phylogenetics and Evolution* 57(3):1091–104.
1430   https://doi.org/10.1016/j.ympev.2010.10.003

1431 Zhao EM, Adler K. 1993. *Herpetology of China.* Published by Society for the Study of
1432   Amphibians and Reptiles.

1433 Zhao EM, Zhao KT, Zhou KY. 1999. *Fauna Sinica. Reptilia. Vol. 2. Squamata. Lacertilia.*
1434   Beijing: Science Press 394.

1435 Zheng H, Wei X, Tada R, Clift PD, Wang B, Jourdan F, Wang P, He M. 2015. Late Oligocene-
1436   early Miocene birth of the Taklimakan Desert. *Proceedings of National Academy of*
1437   *Sciences USA* 112(25):7662-7667. https://doi.org/10.1073/pnas.1424487112

1438

Uncorrected *p*-distances for concatenated sequences of nuDNA (above diagonal) and mtDNA genes (below diagonal) (%) for species groups of *Phrynocepahlu*s (1–11).

Values on the diagonal correspond to average uncorrected ingroup *p*-distances for mtDNA\nuDNA genes (%), respectively.

#	Group	1	2	3	4	5	6	7	8	9	10	11
1	*arabicus-maculatus*	**11.33/0.70**	2.70	3.00	3.00	3.00	2.10	3.50	2.80	3.14	2.99	3.70
2	*interscapularis*	17.71	**11.45/1.57**	3.40	3.60	3.60	2.50	3.60	3.40	3.40	3.39	3.81
3	*scutellatus*	17.96	18.79	—	3.77	3.67	2.80	3.94	3.87	3.63	3.56	3.99
4	*ocellatus*	17.08	17.24	18.54	**7.09/1.00**	1.52	2.50	1.57	2.90	1.73	1.56	2.00
5	*strauchi*	16.45	16.28	18.40	11.92	—	2.40	1.60	2.82	1.57	1.53	2.00
6	*mystaceus*	17.50	17.90	18.73	14.65	13.77	**7.36/0.4**	2.40	2.46	2.37	2.05	2.60
7	*helioscopus*	18.08	17.68	18.99	14.81	14.14	15.64	**11.09/1.14**	2.92	1.77	1.67	2.07
8	*Oreosaura*	16.47	16.08	18.09	14.26	13.59	15.04	14.80	**7.93/0.75**	2.85	2.50	3.16
9	*axillaris*	16.91	16.79	18.24	14.53	12.72	13.98	13.47	13.52	**2.18/—**	1.08	1.75
10	*versicolor*	16.89	16.89	18.12	14.65	13.21	15.78	15.03	13.65	13.64	**6.95/0.31**	0.60
11	*guttatus*	16.92	17.01	18.27	14.40	13.10	15.16	14.91	13.69	13.48	9.28	**5.84/0.58**

Figure 1

Current distribution and species richness of the genus *Phrynocephalus*.

Color indicates the number of sympatric species of *Phrynocephalus* (from one to over four).
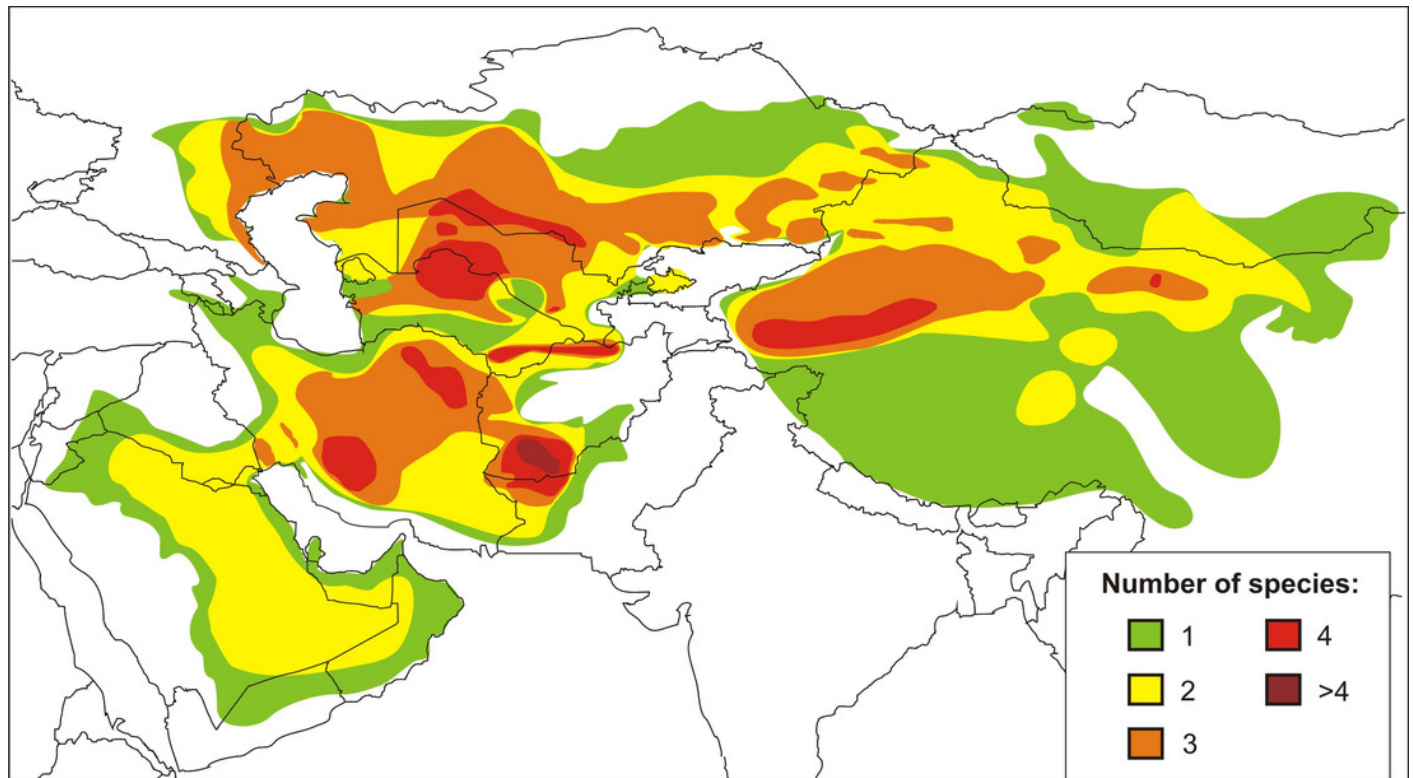
Figure 2

Mitochondrial genealogy of the genus *Phrynocephalus* on the base of 2703 bp (partial *COI*, *Cytb*, *ND2*, *ND4* sequences).

Node support values are given for ML BSP/MP BSP/BI BPP, respectively. Color marking of species groups corresponds to Fig. 3 and Supplementary Fig. S4.
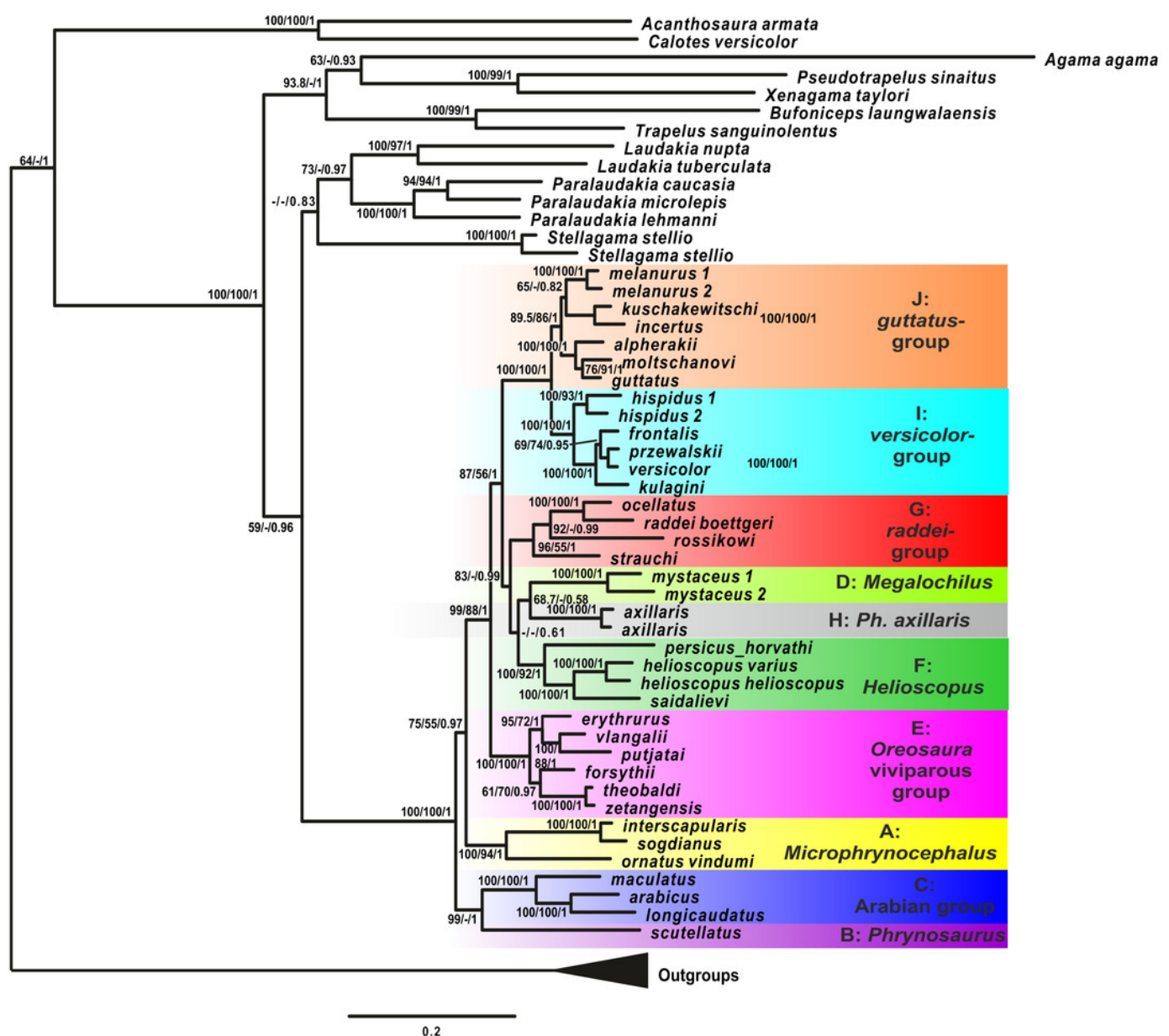
Figure 3

Phylogenetic ML tree reconstructed from concatenated alignment of the nuclear genes *RAG-1*, *BDNF*, *AKAP9* and *NKTR*.

Numbers on tree nodes indicate bootstrap values (BS) and posterior probabilities for ML BSP/MP BSP/BI BPP, respectively. Color marking of species groups corresponds to mitochondrial lineages; see Fig. 2 and Supplementary Fig. S4. Thumbnails show representative species of each *Phrynocephalus* species group (to scale; note large size of *P. mystaceus*). Photographs by E.A. Dunayev and R.A. Nazarov.
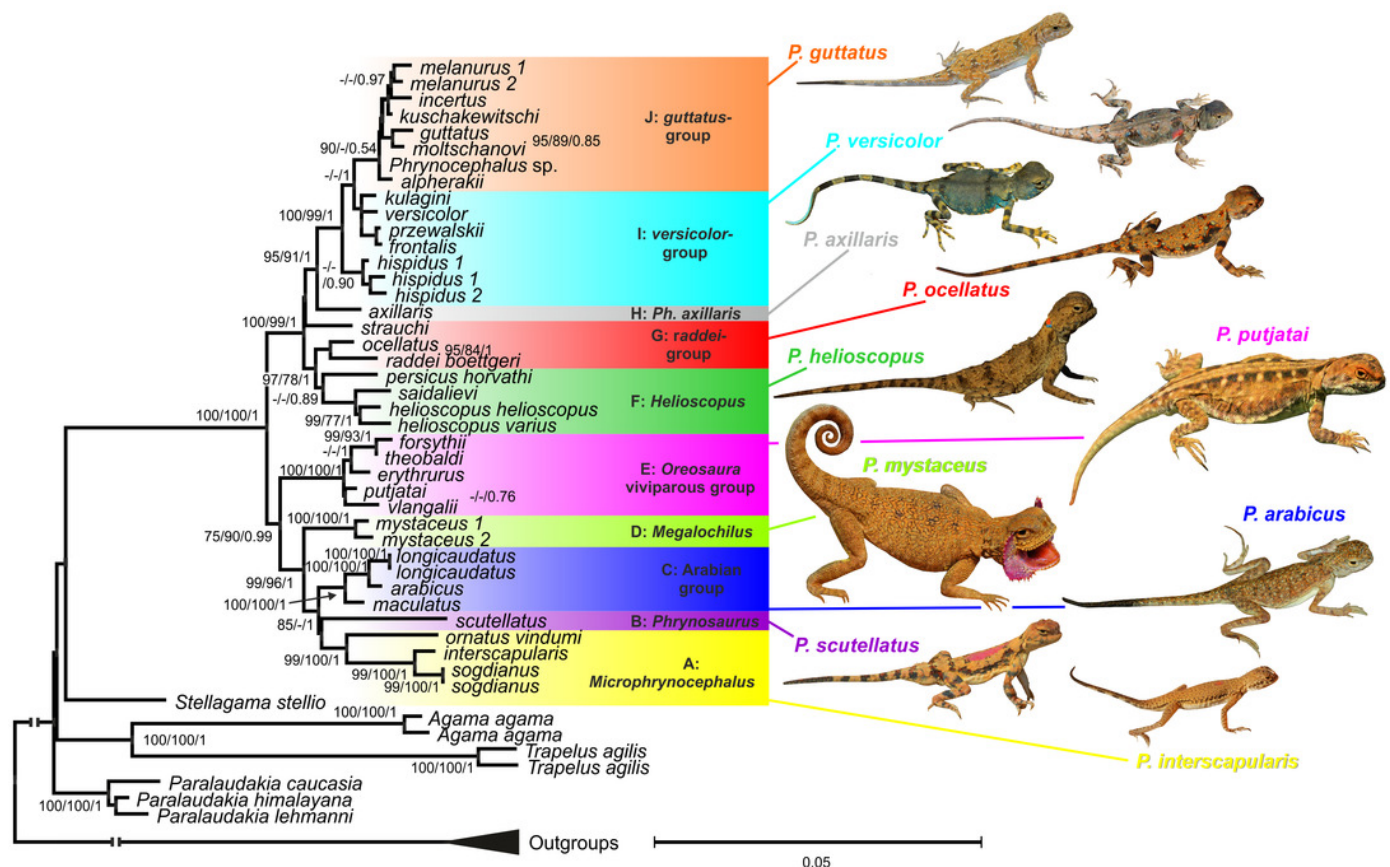
Figure 4

Species tree reconstructed by *BEAST analysis with the nuclear genes *RAG-1*, *BDNF*, *AKAP9* and *NKTR*.

Bayesian posterior probabilities (BI BPP) values are given only for strongly supported nodes. For Clades I–III definitions see Discussion.
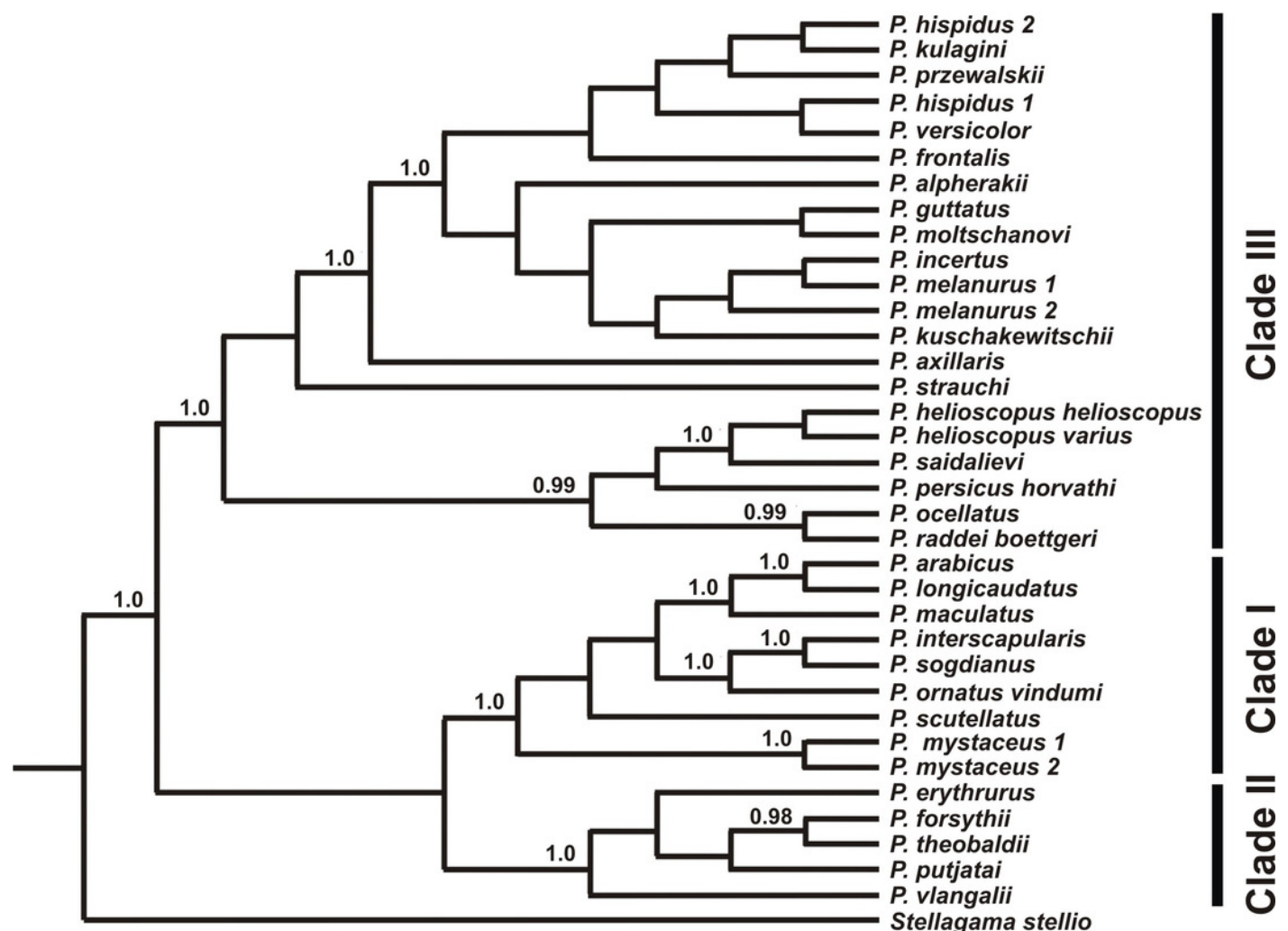
Figure 5

Differentiation of *Phrynocephalus*: BEAST chronogram on the base of nuDNA dataset with results of ancestral area modeling in Lagrange.

Abbreviations: GLB – "*Gomphotherium*-landbridge"; MMTO – Middle Miocene thermal optimum; MMCT – Middle Miocene climatic transition; PPCO – Pliocene-Pleistocene climate oscillations; AR – Near East and Arabia, MI –Asia Minor and Transcaucasia; KZ – Kazakhstan, North Caspian and Ciscaucasian deserts; CA – Central Asia; TU – Turan; TI – Tibet; ME – Middle East. For biogeographic areas definitions see Supplementary File 2 and Supplementary Table S10. For paleogeographic reconstruction see Fig. 6. Node values correspond to estimated divergence times (in Ma). Icons illustrate vicariant events, area expansion and local extinctions, respectively. Black line on the inset shows modern range of *Phrynocephalus*. Red line corresponds to temperature change during the Cenozoic; climatogram from Zachos *et al.* 2001.
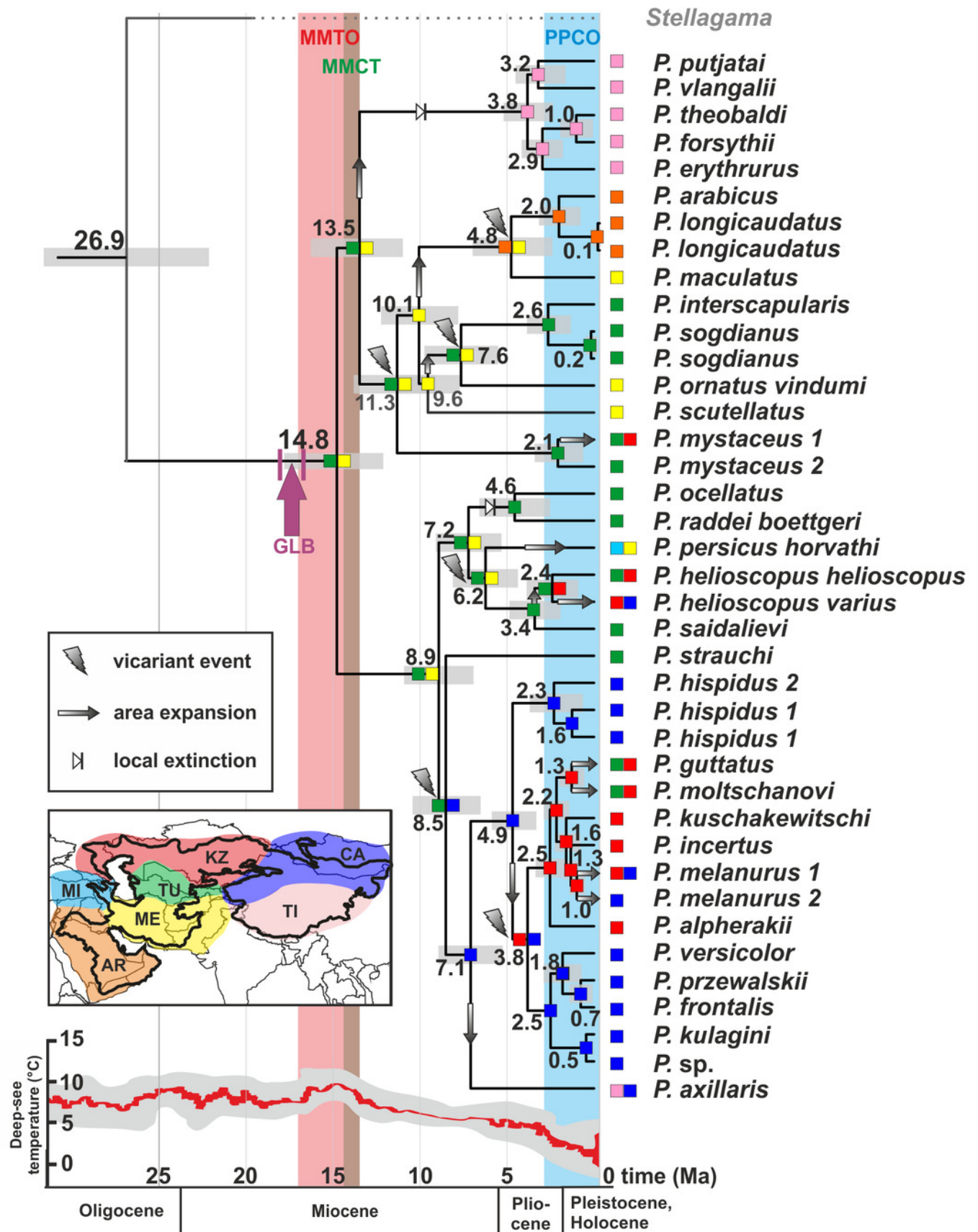
Figure 6

Paleogeography of Paratethys basin in late Cenozoic and the hypothetical scenario for *Phrynocephalus.*

Paleogeographic reconstructions are based on Rögl 1999; Popov et al. 2004; Popov et al. 2009 for early (A) and middle (B) Miocene and Pliocene (C). Question marks denote possible areas of distribution of the common ancestor of Phrynocephalus. GLB – "*Gomphotherium*-landbridge" between Arabian plate and Asian mainland (18–17 Ma). Red dotted line – possible range of *Phrynocephalus*; red arrows – possible dispersal routes; Latin numbers correspond to hypothetical distribution of main Phrynocephalus Clades I–III (see Discussion).
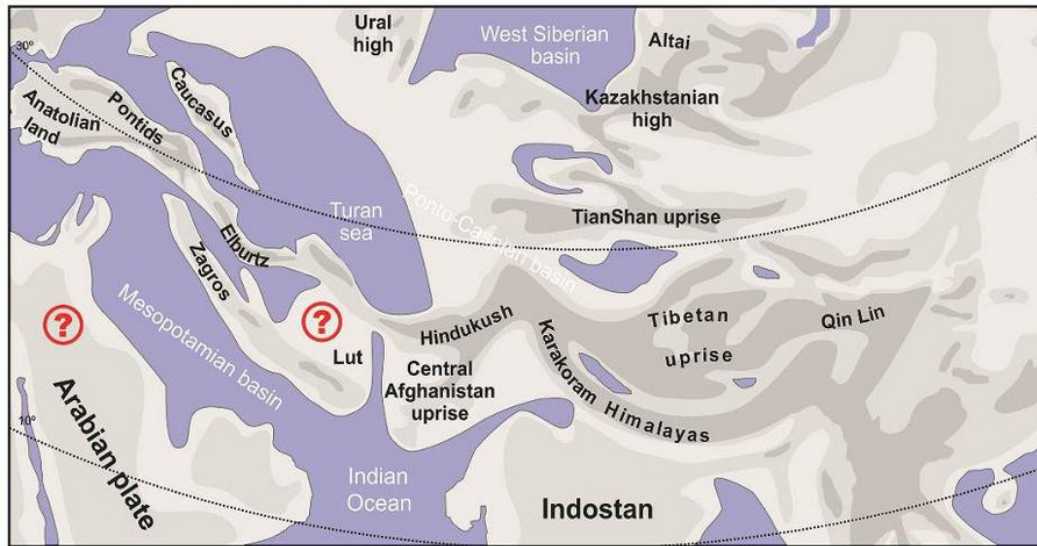
A. Miocene 20-19 Ma

B. Miocene 15-13 Ma
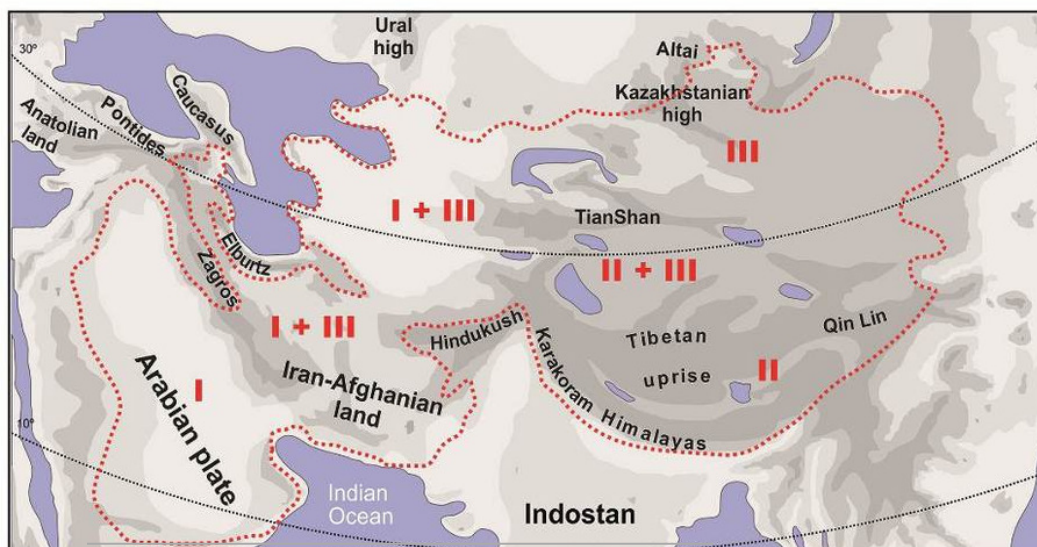
C. Pliocene 3.4-1.8 Ma

Figure 7

Evolution of habitat preference in the Agaminae including the genus *Phrynocephalus*.

See Materials and Methods section and Supplementary Table S5 for habitat data and Supplementary Table S6 for step-matrix showing transition between substrate niche states. Agaminae outgroups, except for *Xenagama*, *Trapelus* and *Bufoniceps*, inhabit large rocks and cliffs. Two lineages within the subfamily independently adapted to sandy habitats: the common ancestor of *Bufoniceps* and *Trapelus* and the ancestor of *Phrynocephalus*. Main groups within *Phrynocephalus* evolved adaptations to life on large loose sand dunes (*P. arabicus*, *P. mystaceus* and *Microphrynocephalus*), stony and gravel highland deserts (subgenus *Oreosaura*) and on clay substrates with gravel (*P. helioscopus–P. raddei* group).
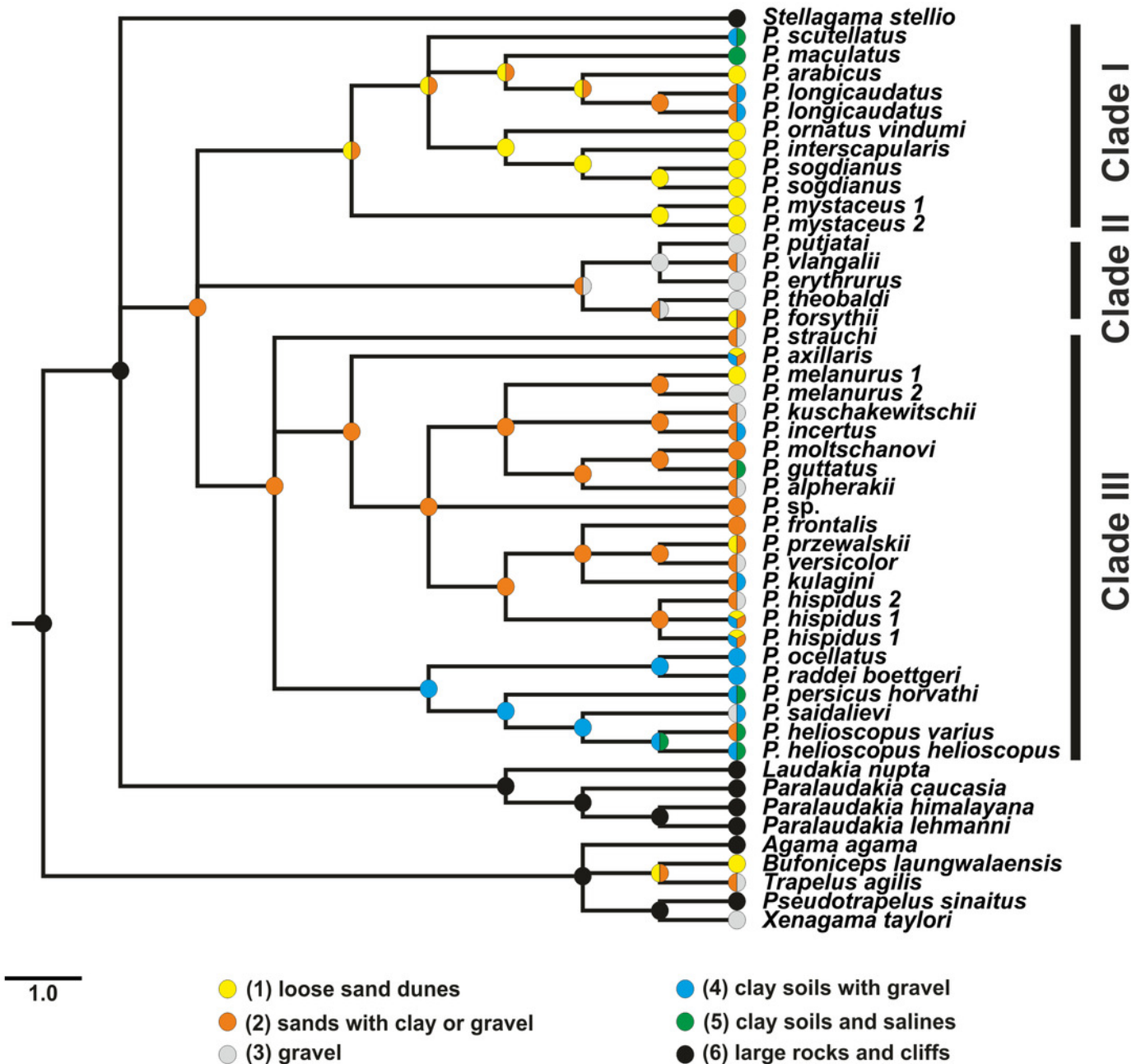
Figure 8

Body-size evolution among Agaminae including genus *Phrynocephalus*.

See Supplementary Table S5 for maximum SVL data. Color of branches corresponds to SVL_{max} (see legend). Rock-dwelling *Laudakia* s.l. are characterized by larger body size, while the common ancestor of *Phrynocephalus* was likely smaller than other Agaminae; sand-dwelling *Microphrynocephalus* (*P. ornatus*–*P. interscapularis* group) and *Megalochilus* (*P. mystaceus* group) represent the most miniaturized and the largest lineages within the genus, respectively.